

RIGA TECHNICAL UNIVERSITY

Oskars OZOLIŅŠ

**ANALYSIS AND REALIZATION OF WAVELENGTH FILTERS IN
FIBER OPTIC TRANSMISSION SYSTEMS**

Summary of the promotion work

Riga 2013

RIGA TECHNICAL UNIVERSITY
Faculty of Electronics and Telecommunication
Institute of Telecommunications

Oskars OZOLIŅŠ
Doctoral student of the programme “Telecommunications”

**ANALYSIS AND REALIZATION OF WAVELENGTH FILTERS IN
FIBER OPTIC TRANSMISSION SYSTEMS**

Summary of the promotion work

Scientific adviser
Dr.sc.eng., Professor
G. IVANOVŠ

RTU Publishing House
Riga 2013

UDK 621.372.852 (043.2)
Oz 640 a

Ozoliņš O. Analysis and Realization of
Wavelength Filters in Fiber Optic Transmission
Systems. Summary of the Promotion Work.-
R.:RTU, 2013.-41 pp.

This work has been supported by the European
Social Fund within the project “Support for the
implementation of doctoral studies at RTU”

Printed according to the decision of the RTU
ETF Promotion Council “RTU P-08” of 21st of
february, 2013, Protocol No. 14.



European Social Fund



European Union

ISBN 978-9934-10-409-1

**PROMOTION WORK
SUBMITTED FOR THE DEGREE OF A DOCTOR OF
ENGINEERING SCIENCES (TELECOMMUNICATIONS) TO BE
DEFENDED AT THE RIGA TECHNICAL UNIVERSITY**

The promotion work for a doctor's degree of engineering sciences (telecommunications) is to be defended publicly at 16:30, on May 23, 2013, at the Faculty of Electronics and Telecommunications of the Riga Technical University, 12 Azenes Str., in the lecture-room No. 210.

OFFICIAL REVIEWERS

Professor Dr.sc.ing. Guntars Balodis
Riga Technical University, Faculty of Electronics and Telecommunications

Professor, Dr.habil.phys. Jānis Spīgulis
University of Latvia, Faculty of Physics and Mathematics

Senior researcher, Dr.phys. Juris Zvirgzds
University of Latvia, Institute of Solid State Physics

CONFIRMATION

I confirm that I have developed this promotion work for a doctor's degree of engineering sciences which is submitted to consideration at the Riga Technical University. The promotion work is not submitted to any other university for receiving a scientific degree.

Oskars Ozoliņš (Signature)

Date: 23.05.2013

This promotion work is written in the Latvian language. It contains Introduction, 4 Chapters, Conclusion, and Bibliography, 5 appendices, 84 figures and illustrations, with the total number of 143 pages. The Bibliography has 164 titles.

GENERAL DESCRIPTION OF THE WORK

Topicality of the subject matter

The rapid rise in the total amount of user data – 32% every year and 82.56 PB monthly by 2016 according to the Cisco forecast (see Fig. 1) [16] – dictates the necessity of searching after new solutions for improvement of the parameters of optical transmission systems. In the world, a tendency is observed to gradually pass from 10 Gbit/s data transmission speed per channel in the wavelength division multiplexing (WDM) systems to 40 Gbit/s and 100 Gbit/s data transmission speed per channel [30]. The basic elements of WDM systems are wavelength filters, which ensure fulfilment of some definite functions: the separation, adding, dropping, and routing of the wavelength range. The wavelength filters could be either those adapted from well-known optical elements (for example, diffraction gratings (DGs) or thin-film filters (TFFs)) or specific devices of planar integrated optics (e.g., arrayed waveguide gratings (AWGs), microring resonators (MRRs)), as well as the filters closely connected with the optical fiber structure (e.g., fiber Bragg gratings (FBGs)).

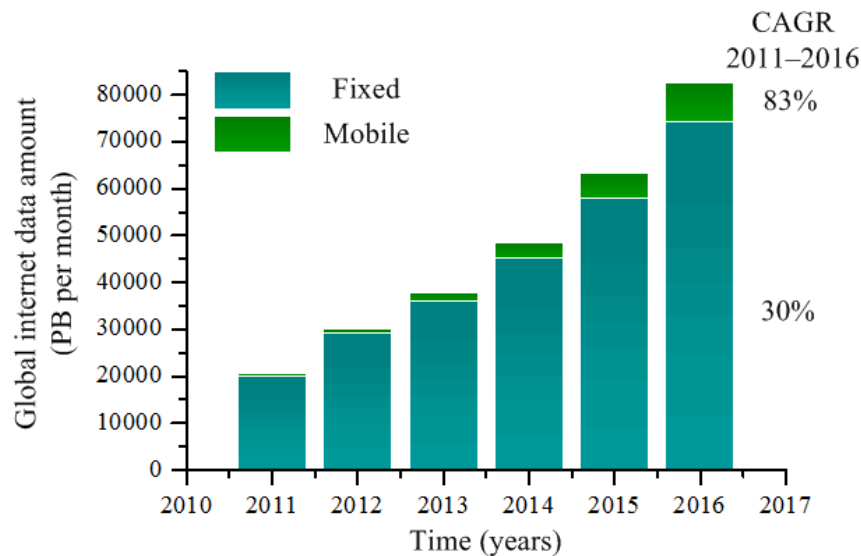


Fig.1. Global internet consumer data amount („Cisco” forecast [16])

In view of rapidly increasing transmission speed in WDM systems the selection among the parameters of a wavelength filter is highly important, since its phase transfer function can be a source of considerable degradation for high-speed optical signals [12, 35, 41]. Besides, taking into account the demand for ever increasing data amount, it is necessary to seek for new solutions as to application of wavelength filters in order to raise the efficiency of WDM systems. One of such solutions could be all-optical conversion of the optical signal's modulation format, thus raising the effectiveness of signal processing and promoting the total system's scalability.

The aim and tasks of the work

Generalizing the facts mentioned above, the **aim of the promotion work** is to estimate theoretically and experimentally the influence of complex transfer characteristics of wavelength filters on the parameters of a WDM and its efficiency.

To achieve the set aim, the following **main tasks** were to be solved:

1. To reveal the most widely used wavelength filters and their parameters as refer to WDM systems as well as to perform the relevant comparative analysis in dependence on the physical realization.

2. To generalize the analytical, numerical and measurement methods for determination of complex transfer function of wavelength filters and to obtain such functions for FBG, TFF, DG, AWG and MRR filters, as well as to create the algorithm of processing and verifying the obtained complex transfer functions in the WDM simulation block diagrams.
3. To work out the methods for checking the effective bandwidth of a wavelength filter and to find out the effective bandwidth of the selected wavelength filters for the 2.5 Gbit/s and 10.3125 Gbit/s NRZ-OOK optical signals.
4. To work out a method for estimation of the possibility to improve the spectral efficiency of 2.5 Gbit/s and 10.3125 Gbit/s NRZ-OOK WDM systems, having preserved the existing wavelength filter technology.
5. To estimate the most effective complex transfer function for separation of optical signals in dense WDMs depending on the channel's data transmission speed (2.5 Gbit/s 10 Gbit/s and 40 Gbit/s), the inter-channel spacing (50 GHz, 100 GHz and 200 GHz) and the type of coding the optical signal.
6. To work out the prototype of a microring resonator (MRR) for the channel separation and find out the influence of MRR cascade on the 40 Gbit/s CSRZ-OOK and CSRZ-DPSK optical signals, as well as a similar MRR prototype for conversion of OOK and DPSK modulated optical signals from RZ to NRZ.

The methodology of research

In realization of the mentioned tasks and in analysis of the relevant problems, in the promotion work the mathematical calculations, numerical simulations, and experimental measurements were employed. The mathematical description of wavelength filters is performed using complex transfer functions, with the phase transfer function derived from the amplitude square transfer function using the Hilbert transformation. In the numerical simulations the nonlinear Schrödinger equation was used along with direct and inverse fast Fourier transform, and the Monte-Carlo method for the BER determination. To obtain the complex characteristics of wavelength filters different measurement methods were employed. The amplitude square curves were obtained by the tunable laser method and the broadband light source method; in turn, the phase transfer function, group delay and dispersion are obtained using the modulated phase shift method. For the optical signal quality estimation, the measurements of power spectrums, eye diagrams and bit error ratios were performed.

The results and scientific novelty of the research

The scientific novelty of the promotion work consists in the following:

1. A method has been worked out for determination of the wavelength filter's effective bandwidth in the limits of which the transmitted optical signal preserves $BER < 10^{-9}$, so as to improve the ITU-T G.671 recommendation for the transmission parameters of optical components and subsystems.
2. The RZ-NRZ conversion of the 41.6 Gbit/s DPSK optical signals has been performed theoretically and experimentally, using a single-ring MRR filter as well as the simultaneous RZ-NRZ conversion of 41.6 Gbit/s OOK and DPSK optical signals using a single-ring MRR filter.

During the implementation of the promotion work the following **main conclusions** have been obtained:

1. The developed algorithm allows for processing of the theoretically & experimentally obtained complex transfer functions of wavelength filters (FBG, TFF, diffraction gratings, AWG, MRR) and for creation of user-defined filter models, thus making it possible to introduce a set of wavelength filter models into the simulation programs.
2. The proposed measuring method is suitable for evaluation of the effective bandwidth of wavelength filters. It is found that in the case of FBG filters the effective bandwidth

decreases by half at a higher transmission speed, which is explained by a greater introduced dispersion as compared with TFF. In turn, in the TFF case the effective bandwidth is stable at 2.5 Gbit/s and 10.3125 Gbit/s transmission speed.

3. In the 10.3125 Gbit/s DWDM systems the spectral efficiency in the case of a 200 GHz TFF could be raised twice (from 0.05 bit/s/Hz to 0.1 bit/s/Hz), while in the 100 GHz TFF case – from 0.1 bit/s/Hz to 0.14 bit/s/Hz.
4. A higher quality of the signal could be achieved with Supergaussian and Raised Cosine filters. In the case of a Raised Cosine filter a better signal quality is observed at a lower transmission speed, which is connected with a greater group delay than in the case of a Supergaussian filter. In turn, with a Raised Cosine filter it is also possible to perform a phase-to-intensity conversion of the modulation format. Such a solution – as compared with Supergaussian and Lorentzian filters – is better from the viewpoint of resistance against the bandwidth decrease caused by the cascade.
5. For the 40 Gbit/s CSRZ-OOK and CSRZ-DPSK optical signals after five cascaded single-ring MRR filters $BER < 10^{-9}$ has been achieved. The CSRZ-OOK modulation format is more stable against the filtering effects as compared with the CSRZ-DPSK modulation format, since in the latter a partial phase-to-intensity conversion occurs with a decreasing MRR bandwidth at five cascaded filters.
6. Using a single-ring MRR filter it is possible to perform the modulation format conversion from RZ-DPSK to NRZ-DPSK and simultaneous RZ-NRZ conversion of the OOK and DPSK optical signals; in particular, this has been realized at the 41.6 Gbit/s transmission speed.

Practical value of the work

1. The research results of the promotion work have been employed for realization of five international and eight Latvian scientific research projects and are to be used for development of the European fund project Nr.3DP/3.2.2.3.0/12/IPIA/SM/001 „Next generation electronic communication network development in countryside”.
2. The recommendations elaborated during fulfilment of the work are envisaged both for improvement of the operating WDM systems and for implementation of new ones. In the framework of a cooperation agreement these have already been put into practice at the J/S „Latvenergo” Co., J/S Ltd „Telia Latvia” Co., and J/S Ltd „TELE2” Co. for investigation and implementation of such type systems.
3. A measuring scheme (patented in Latvia) has been worked out in order to check the effective bandwidth of a wavelength filter for 2.5 Gbit/s and 10.3125 Gbit/s NRZ-OOK optical signals.
4. A two-channel measuring scheme (patented in Latvia) has been created for 2.5 Gbit/s and 10.3125 Gbit/s NRZ-OOK optical signals with the aim to estimate the possibility of raising the spectral efficiency of WDM system, having preserved, at the same time, the existing wavelength filter technology.

The theses to be defended:

1. The developed method allows determination of the effective bandwidth of a wavelength filter in the limits of which the transmitted optical signal keeps $BER < 10^{-9}$. In the criteria defined by ITU-T G.671 recommendation for determination of the wavelength filter bandwidth its influence on the optical signals' quality is ignored.
2. Using the elaborated method it is possible to improve the spectral efficiency of a WDM system by reducing the inter-channel space up to the minimum, preserving at the same time the existing wavelength filter technology. The manufacturers of wavelength filters specify their passband widths at minus 3 dB, not however defining for what intervals between channels and what transmission speeds these are implied.

3. For the 40 Gbit/s CSRZ-OOK and CSRZ-DPSK optical signals after five cascaded single-ring MRR filters the BER value $<10^{-9}$ is achievable. Greater signal distortions are observed for the 40 Gbit/s CSRZ-DPSK optical signals due to the partial phase-intensity conversion of the modulation format.
4. Using a single-ring MRR filter it is possible to perform simultaneously the RZ-NRZ conversion of 41.6 Gbit/s OOK and DPSK optical signals with preserving BER $< 10^{-9}$.

Approbation of the results of the research

The main results of the promotion work are presented at **20** international scientific conferences; these are reported in **10** publications in scientific journals, **6** publications in the full-text conference proceedings, **8** publications in the conference books of abstracts, and **2** Latvian patents.

Reports at the international scientific conferences:

1. Ļašuks I., Ščemeļevs A., **Ozoliņš O.** Investigation of Spectrum-Sliced WDM System // „Electronics 2008”, Lithuania, Kaunas, May 19-23, 2008.
2. **Ozoliņš O.**, Bobrovs V. Investigation Of Flat-Top Bpf Usability In Amplified Fiber Optical Systems // „Development in Optics and Communication 2009”, Latvia, Riga, April 24-26, 2009.
3. **Ozoliņš O.**, Ivanovs Ģ. Realization of optimal FBG band-pass filters for high speed HDWDM // „Electronics 2009”, Lithuania, Kaunas, May 12-13, 2009.
4. **Ozoliņš O.**, Ivanovs Ģ. Evaluation of optimal FBG filter apodization function for HDWDM // „50th RTU Scientific Conference”, Latvia, Riga, October 14-16, 2009.
5. **Ozoliņš O.**, Ivanovs Ģ. Estimation of optical filter narrowing in high speed WDM systems // „Developments in optics and communications 2010”, Latvia, Riga, 23-25 April, 2010.
6. **Ozoliņš O.**, Ivanovs Ģ. Evaluation of Band-Pass Filters Influence on NRZ Signal in HDWDM Systems // „Electronics 2010”, Lithuania, Kaunas, May 18-20, 2010.
7. **Ozoliņš O.**, Bobrovs V. Research of Fiber Bragg Gratings in WDM Technologies for Broadband Access // „Optics & High Technology Material Science 2010”, Ukraine, Kiev, October 21-24, 2010.
8. **Ozoliņš O.**, Ivanovs Ģ. Reaserch of thin film filter for for broadband access systems // „Developments in Optics and Communications 2011”, Latvia, Riga, 28-30 April, 2011.
9. **Ozoliņš O.**, Ivanovs Ģ. Estimation of DWDM transmission for broadband access with FBG technology // „Electronics 2011”, Lithuania, Kaunas, May 17-19, 2011.
10. **Ozoliņš O.**, Bobrovs V., Ivanovs Ģ. Efficient Bandwidth Measurements of Thin Film Filters for Next-Generation Optical Access // „The 12th Annual Post Graduate Symposium on the Convergence of Telecommunications, Networking and Broadcasting 2011”, United Kingdom, Liverpool, June 27-28, 2011.
11. **Ozoliņš O.**, Bobrovs V., Ivanovs Ģ. Investigation of Efficient Bandwidth of FBG filters for Next-Generation Optical Access // „52th RTU Scientific Conference”, Latvia, Riga, October 13-14, 2011.
12. **Ozoliņš O.**, Bobrovs V., Ivanovs Ģ. DWDM-Direct System with 50 GHz FBG for New-Generation Optical Access // „IEEE Swedish Communication Technologies Workshop Proceedings”, Sweden, Stockholm, October 19-21, 2011.
13. **Ozoliņš O.**, Bobrovs V., Ivanovs Ģ. Efficient bandwidth measurements of fiber Bragg gratings for next-generation optical access // „Optics & High Technology Material Science 2011”, Ukraine, Kiev, October 27-30, 2011.
14. **Ozoliņš O.**, Bobrovs V., Ivanovs Ģ. Efficient Bandwidth of 50 GHz Fiber Bragg Grating for New-Generation Optical Access // „19th Telecommunications Forum 2011”, Serbia, Belgrade, November 22-24, 2011.

15. **Ozoliņš O.**, Ivanovs Ģ. New Generation Access System Based On DWDM-Direct With 55 GHz Fiber Bragg Grating // Developments in Optics and Communications 2012, Latvia, Riga, April 12-14, 2012.
16. **Ozoliņš O.**, Bobrovs V., Ivanovs Ģ. DWDM-Direct Access System Based on the Fiber Bragg Grating Technology // 8th International Symposium on Communication Systems, Networks and Digital Signal Processing 2012, Poland, Poznan, July 18-20, 2012.
17. Xiong M., **Ozoliņš O.**, Ding Y., Huang B., An Y., Ou H., Peucheret C., Zhang X. 41.6 Gb/s RZ-DPSK to NRZ-DPSK Format Conversion in a Microring Resonator // 17th OptoElectronics and Communications Conference 2012, South Korea, Busan, July 2-6, 2012.
18. Lali-Dastjerdi Z., **Ozoliņš O.**, An Y., Cristofori V., Da Ros F., Kang N., Hu H., Hansen Mulvad H., Rottwitt K., Galili M., Peucheret C. Demonstration of Cascaded In-Line Single-Pump Fiber Optical Parametric Amplifiers in Recirculating Loop Transmission // European Conference on Optical Communications 2012, Netherlands, Amsterdam, September 16-20, 2012.
19. **Ozoliņš O.**, An Y., Lali-Dastjerdi Z., Ding Y., Bobrovs V., Ivanovs Ģ., Peucheret C. Cascadability of Silicon Microring Resonators for 40 Gbit/s OOK and DPSK Optical Signals // Asia Communications and Photonics Conference 2012, China, Guangzhou, November 7-10, 2012.
20. **[Invited]** Peucheret C., Ding Y., Ou H., Xiong M., An Y., Lorences Riesgo A., Xu J., **Ozoliņš O.**, Hu H., Galili M., Huang B., Pu M., Ji H., Seoane J., Liu L., Zhang X. Linear Signal Processing Using Silicon Micro-Ring Resonators // International Photonics and OptoElectronics Meetings 2012, China, Wuhan, November 1-2, 2012.

Publications in scientific journals:

1. Ļašuks I., Ščemeļevs A., **Ozoliņš O.** Investigation of Spectrum-Sliced WDM System // Electronics and Electrical Engineering. - 5. (2008) 45.-48. p.
2. **Ozoliņš O.**, Ivanovs Ģ. Realization of Optimal FBG Band-Pass Filters for High Speed HDWDM // Electronics and Electrical Engineering. - 4. (2009) 41.-44. p.
3. Bobrovs V., **Ozoliņš O.**, Ivanovs Ģ. Investigation into the Potentialities of Quasi-Rectangular Optical Filters in HDWDM Systems // Latvian Journal of Physics and Technical Sciences. - 1. (2010) 13.-25. p.
4. Ivanovs Ģ., Bobrovs V., **Ozoliņš O.**, Poriņš J. Realization of HDWDM Transmission System // International Journal of Physical Sciences. - 5. (2010) -452.-458. p.
5. **Ozoliņš O.**, Bobrovs V., Ivanovs Ģ. Efficient Wavelength Filters for DWDM Systems // Latvian Journal of Physics and Technical Sciences. - 6. (2010) 47.-58. p.
6. **Ozoliņš O.**, Ivanovs Ģ. Evaluation of Band-Pass Filters Influence on NRZ Signal in HDWDM Systems // Electronics and Electrical Engineering. - 4. (2010) 65.-68. p.
7. **Ozoliņš O.**, Bobrovs V., Ivanovs Ģ. DWDM Transmission Based on the Thin-Film Filter Technology // Latvian Journal of Physics and Technical Sciences. - 3. (2011) 55.-65. p.
8. **Ozoliņš O.**, Ivanovs Ģ. Estimation of DWDM Transmission for Broadband Access with FBG Technology // Electronics and Electrical Engineering. - 5. (2011) 11.-14. p.
9. **Ozoliņš O.**, Bobrovs V., Ivanovs Ģ., Ļašuks I. New-Generation Optical Access System Based on the Thin Film Filter Technology // International Journal of the Physical Sciences. - 6(35). (2011) 7926.-7934. p.
10. Xiong M., **Ozoliņš O.**, Ding Y., Huang B., An Y., Ou H., Peucheret C., Zhang X. Simultaneous RZ-OOK to NRZ-OOK and RZ-DPSK to NRZ-DPSK format conversion in a silicon microring resonator // Optics Express (2011 ISI Impact Factor: 3.587). - Vol.20, No.5,. (2012) 27263.-27272. p.

Publications in the full-text conference proceedings:

1. **Ozoliņš O.**, Bobrovs V., Ivanovs Ģ. Efficient Bandwidth Measurements of Thin Film Filters for Next-Generation Optical Access // PGNet2011 Conference Proceedings, United Kingdom, Liverpool, June 27-28, 2011. - 275.-280. p.
2. **Ozoliņš O.**, Bobrovs V., Ivanovs Ģ. Efficient Bandwidth of 50 GHz Fiber Bragg Grating for New-Generation Optical Access // 19th IEEE Telecommunications Forum TELFOR 2011 IEEE Catalog number: CFP1198P-CDR, Serbia, Belgrade, November 22-24, 2011. - 816.-819. p.
3. **Ozoliņš O.**, Bobrovs V., Ivanovs Ģ. DWDM-Direct Access System Based on the Fiber Bragg Grating Technology // 8th International Symposium on Communication Systems, Networks and Digital Signal Processing (CSNDSP'12): Proceedings, Poland, Poznan, July 18-20, 2012. - 1.-4. p.
4. Xiong M., **Ozoliņš O.**, Ding Y., Huang B., An Y., Ou H., Peucheret C., Zhang X. 41.6 Gb/s RZ-DPSK to NRZ-DPSK Format Conversion in a Microring Resonator // 17th Opto-Electronics and Communications Conference (OECC 2012): Technical Digest, South Korea, Busan, July 2-6, 2012. - 891.-892. p.
5. Lali-Dastjerdi Z., **Ozoliņš O.**, An Y., Cristofori V., Da Ros F., Kang N., Hu H., Hansen Mulvad H., Rottwitt K., Galili M., Peucheret C. Demonstration of Cascaded In-Line Single-Pump Fiber Optical Parametric Amplifiers in Recirculating Loop Transmission // European Conference on Optical Communications (ECOC) 2012: Proceedings, Netherlands, Amsterdam, September 16-20, 2012. - 1.-3. p.
6. **Ozoliņš O.**, An Y., Lali-Dastjerdi Z., Ding Y., Bobrovs V., Ivanovs Ģ., Peucheret C. Cascadability of Silicon Microring Resonators for 40 Gbit/s OOK and DPSK Optical Signals // Asia Communications and Photonics Conference (ACP) 2012: Proceedings, China, Guangzhou, November 7-10, 2012. - 1.-3. p.

Publications in the conference books of abstracts:

1. **Ozoliņš O.**, Bobrovs V. Investigation of Flat-Top BPF Usability in Amplified Fiber Optical Systems // Developments in Optics and Communications 2009 Book of Abstracts, Latvia, Riga, April 24-26, 2009. - 24-24.p.
2. **Ozoliņš O.**, Ivanovs Ģ. Estimation of Optical Filter Narrowing in High Speed WDM Systems // Developments in Optics and Communications 2010 Book of Abstracts, Latvia, Riga, April 23-25, 2010. - 41.-41.p.
3. **Ozoliņš O.**, Bobrovs V. Research of Fiber Bragg Gratings in WDM Technologies for Broadband Access // Optics & High Technology Material Science SPO 2010 Scientific works, Ukraine, Kiev, October 21-24, 2010. - 158.-159. p.
4. **Ozoliņš O.**, Bobrovs V., Ivanovs Ģ. Evaluation of Optical Filters for DWDM-Direct in Next Generation Optical Access // Developments in Optics and Communications 2011 Book of Abstracts, Latvia, Riga, April 28-30, 2011. - 42.-43. p.
5. **Ozoliņš O.**, Bobrovs V., Ivanovs Ģ. Efficient bandwidth measurements of fiber Bragg gratings for next-generation optical access // Optics & High Technology Material Science SPO 2011 Scientific works, Ukraine, Kiev, October 27-30, 2011. - 233.-234. p.
6. **Ozoliņš O.**, Bobrovs V., Ivanovs Ģ. DWDM-Direct System with 50 GHz FBG for New-Generation Optical Access // IEEE Swedish Communication Technologies Workshop Conference Proceedings, Sweden, Stockholm, October 19-21 2011. - 10.-10. p.
7. **Ozoliņš O.**, Ivanovs Ģ. New Generation Access System Based On DWDM-Direct With 55 GHz Fiber Bragg Grating // Developments in Optics and Communications 2012: Book of Abstracts, Latvia, Riga, April 12-14, 2012. - 80.-81. p.
8. Peucheret C., Ding Y., Ou H., Xiong M., An Y., Lorences Riesgo A., Xu J., **Ozoliņš O.**, Hu H., Galili M., Huang B., Pu M., Ji H., Seoane J., Liu L., Zhang X. **[Invited]** Linear Signal Processing Using Silicon Micro-Ring Resonators // International Photonics and

OptoElectronics Meetings (POEM 2012-IONT): Proceedings, China, Wuhan, November 1-2, 2012. - 1.p.

Latvian patents:

1. Measuring scheme for evaluation of efficient bandwidth of wavelength filter, LV-14557, 2012;
2. Wavelength division multiplexing transmission system with narrow-band filter, LV-14107, 2009;

The results of the promotion work were used for realization of 5 International and 8 Latvian scientific research projects realization:

International scientific research projects:

1. „Next generation mixed optical wavelength division multiplexing system enforcement.”, Nr. EEZ09AP-42/09, EEZ grant.
2. National Basic Research Program of China, Grant No. 2011CB301704.
3. National Natural Science Foundation of China, Grant No. 61007042.
4. 7th framework program of the European Commission DAPHNE project, ref. 233709.
5. 7th framework program of the European Commission Network of excellence EURO-FOS project, ref. 224402.

Latvian scientific research projects:

1. „Development of mixed fiber optical wavelength division multiplexing transmission system.”, No. FLPP-2011/15, RTU;
2. „Investigation of nonlinear optical coefficient measurement method in FOTS”. No. ZP 2010, RTU;
3. „Investigation of optical signal polarization state determination methods in FOTS.”, No. ZP2009/6, RTU;
4. „New electronic communication technologies”, the National Research Programme deviation - The Telecommunications system safety and security, No. V7408.1, RTU;
5. „Investigation of IP over WDM traffic grooming”, No. ZP 2008/16, RTU;
6. „Investigation of traffic control in FTTH networks”, No. ZP 2007/13, RTU;
7. „High-speed optical WDM systems development and evaluation.”, No. R7365, RTU;
8. „Research of spectrally multiplexed broadband passive optical network implementation possibilities” No. ZP-2009/L-27, RTU;

The volume and structure of the work

The volume of the promotion work is 143 pages. The work consists of the introduction, four chapters, the list of literature sources used, and four appendices. In the introduction, the topicality of the carried out research is substantiated and the promotion work direction defined.

In Chapter 1, the developmental tendencies are overviewed for the wavelength filters and a comparative analysis performed for their most widely applied physical realizations in WDM systems. Apart from that, formulated are the aim and tasks of the promotion work, its scientific novelty, the theses to be defended; the main its results are generalized and the directions of further research defined.

In Chapter 2, the mathematical description of the wavelength filters is given, and the measuring methods for determination of their complex transfer function are overviewed. The measurements of the the complex transfer function are described along with the algorithm worked out for processing this function (obtained both theoretically and experimentally) as well as for creation of a user-defined filter of the type in OptSim program.

In Chapter 3, description is presented as to the developed and patented in Latvia measuring scheme for determination of the wavelength filter effective bandwidth as well as the developed and patented in Latvia measuring scheme for estimation of the possibility to improve the WDM spectral efficiency while preserving the wavelength filter technology. Next, in this chapter the procedure of determination of the most effective complex transfer function for a dense WDM system is described, along with determination of a wavelength filter's bandwidth values to be used for the phase-to-intensity modulation format conversion using the Lorentzian, Raised Cosine, and Supergaussian filters.

In Chapter 4, an overview is given for a new-type wavelength filter, namely, a micro-ring resonator, which so far has not been applied in commercial WDM systems. The relevant investigation described in this chapter was done during the doctoral studies' practice at the Technical University of Denmark, Department of Photonics Engineering, ETDM Laboratory, in cooperation with the scientists from the laboratory of the Wuhan National Optoelectronic and under the supervision of Professor Christophe Peucheret. In this chapter, the influence of cascading the MRR filters on the 40 Gbit/s OOK and DPSK modulation formats is considered alongside the successful RZ-NRZ conversion of 41.6 Gbit/s phase-modulated optical signals, as well as with simultaneous RZ-NRZ conversion of 41.6 Gbit/s intensity- and phase-modulated optical signals.

In the summary, the main conclusions are presented. In the appendices present lists of the conferences, the publications and the projects, the data on the Latvian patents, the recommendation about doctoral studies' practice and specification on used equipment.

DETAILED DESCRIPTION OF THE WORK'S CHAPTERS

Chapter 1

The information and communication technologies are progressing uninterruptedly [27], with especially rapid progress observed in the last decades. The dominant position in the current data transmission is occupied by fiber optics transmission systems [6]. This is mainly connected with a large bandwidth of single-mode fibers (SMFs) reaching 50 THz and more in the wavelength range from 1200 nm to 1600 nm [47]. To fully exploit this potential there are needed technologies for making WDM systems in which multiple data transmission channels with different wavelengths are concentrated in one SMF. However, it is necessary to separate these channels from each other at the SMF output, which is a challenging task [75].

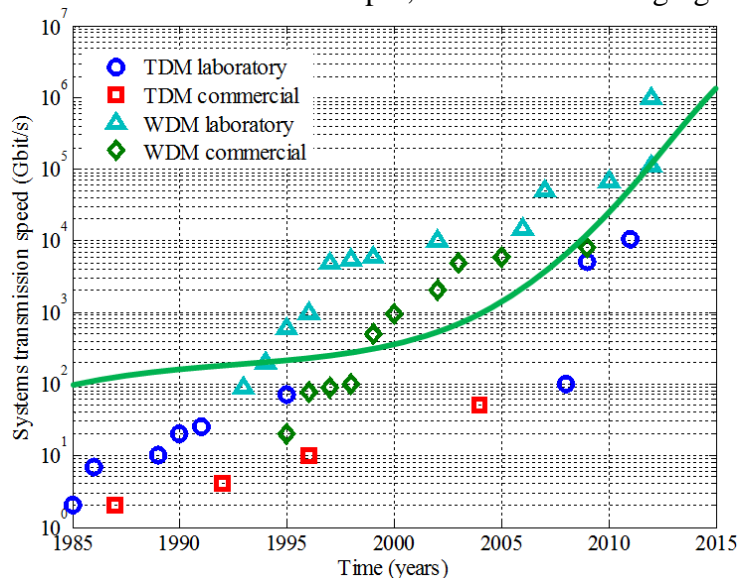


Fig. 2. System's transmission speed and global demand for the amount of data [32]

The research into the WDM as technology gained speed in the 70-ies of the past century; by now, its use has allowed for many-hundred channel transmission through a single optical fiber. In the 90-ies of the 20-th century an erbium-doped field amplifier appeared. Its invention made it possible to considerably extend – in comparison with the fourth-generation fiber optics transmission systems – the optical fiber lines. In parallel with EDFA, the WDM systems were developed, thus allowing for the data transmission speed as high as 10 Gbit/s per channel [4]. Since 1992, the total data amount transmitted through a single optical fiber has been increasing exponentially. While in 2001 it reached 10 Tbit/s [2], in 2010 the level of 69.1 Tbit/s at a transmission distance of 240 km was achieved [69]. These data transmission speeds were gained using SMF as transmission medium. On August 15, 2011, a paper was published in which the total data transmission speed of 112 Tbit/s was reported for a distance of 76.8 km through a single optical fiber [88]. The authors, in addition to the WDM technology, used a spatial multiplexing of new-type multi-core optical fibers. It should be noted that on September 19, 2012, at the „ECOC2012” conference a 1.01 Pbit/s single-fiber transmission was stated [72]. As seen in Fig. 2, the total demand for the data volume is ever increasing. Undoubtedly, the WDM commercial solutions have allowed the appropriate data amounts to be ensured [32]. From the facts mentioned above, today the WDM technology is dominant, making it possible to use the optical fiber’s passband to the ever increasing extent.

With the channel data transmission speed and the number of channels in a WDM system increasing while the inter-channel spacing decreasing, a special attention should be paid to the choice of physical realization and parameters of the wavelength filter [75]. Quite often there should be a compromise between the insertion loss, the quality of adjacent channels’ separation and the induced dispersion. The wavelength filter’s parameters should also be stable against climatic and constructive factors, such as elevated humidity, variations in the working temperature, and diversified mechanical effects [23]. The technologies currently applied in WDM systems for realization of wavelength filters are: TFF, FBG, AWG and diffraction gratings [23, 71, 75]. The TFF, FBG and AWG are wider used in the commercial and already working WDM systems [26, 71, 74]. In turn, the physical filter realization based on diffraction gratings can be done using tunable parameters – e.g. those tuned by wavelengths and so far applied mostly in scientific research [2, 75]. The FBG technology provides good separation of adjacent channels, however requires using the optical circulators, which enlarges the size of device. Therefore, TFF seems to be preferable, since it does not require any additional optical elements [38]. These last two technologies are employed in WDM systems with the number of channels less than 16. In turn, the AWG technology is meant for a greater number of channels (see Table 1). The physical realization of such a wavelength filter was one of the main prerequisites for the development of WDM systems and the more effective utilization of the optical fiber’s passband. As of now, it is impossible to assert that in the transmission systems of the future only one physical realization will be used for wavelength filters; more probable is that in diversified technologies different stages of filtering (cascaded filters) will be combined, thus minimizing the insertion loss and dispersion, with a substantially increasing data transmission speed in a particular channel of the WDM. Therefore, to ensure better effectiveness it is necessary to find out what are limitations imposed by the complex transfer functions of existing wavelength filters in the cases of high transmission speed and great number of users in fiber optics transmission systems – both present and future.

As concerns the phase transfer function of wavelength filters, this could be a source of considerable degradation in the high-speed WDM systems [12, 35, 41]. The phase transfer function has assumed an ever increasing significance with the increasing data transmission speed, which occurs as technological development progresses. First of all, in commercial systems the speed of transmission by one channel has been rapidly increasing; a similar tendency is observed in the access networks based on WDM technologies [45]. Second, with increasing efficiency of WDM systems the channels’ intervals are reduced to the minimum,

which is connected with applying wavelength filters with much narrower band. As a result, in such communication systems also small dispersion values (<100 ps/nm) should be taken into account. In the case when the optical fiber bandwidth (accessible for a particular WDM system's channel) decreases, a detailed analysis is needed to estimate the influence of a wavelength filter on the quality of a transmitted signal. Into consideration also “edges” of the complex transfer function of a wavelength filter should be taken where the dispersion impact is the greatest, since the phase transfer function of wavelength filters is nonlinear in this range. Also a fact should be mentioned – that the wavelength filters with the best isolation of adjacent channels possess the highest dispersion [26, 40, 41]. Therefore, it is especially important to know the degree of the dispersion introduced by wavelength filter in order to avoid possible signal degradation in the systems with rapidly increasing transmission speed.

Table 1.

Comparison of wavelength filters for DWDM systems

Fiber Bragg grating filters	Thin film filters
<ul style="list-style-type: none"> • Insertion loss > 1 dB; • Polarization dependent loss ~ 0.1 dB; • Adjacent channel isolation 30 dB; • Channel interval > 50 GHz; • Temperature dependence 0.5 pm/C^o and unstable from mechanical stress; • Temperature stabilization coating needed; • Architecture 1×1 and channel number enlargement by degrees; • Multiple filters connected in cascade reduces the number of channels < 16; • Simplex in operation if structure is with apodization functions; • Passive devices and used in combination with optical circulators; • Higher dispersion. 	<ul style="list-style-type: none"> • Insertion loss > 1 dB; • Polarization dependent loss ~ 0.2 dB; • Adjacent channel isolation 30 dB; • Channel interval > 50 GHz; • Temperature dependence 0.3 pm/C^o C^o and unstable from mechanical stress; • Temperature stabilization coating needed; • Architecture 1×1 and channel number enlargement by degrees; • Multiple filters connected in cascade reduces the number of channels < 16; • Duplex; • Passive devices; • Small dispersion within the pass band of the filter.
Arrayed waveguide grating filters	Diffraction grating filters
<ul style="list-style-type: none"> • Insertion loss > 5 dB; • Polarization dependent loss ~ 0.5 dB; • Adjacent channel isolation 25 dB; • Channel interval > 50 GHz; • Temperature dependence ~ 10 pm/C^o and unstable from mechanical stress; • Temperature stabilization coating and active temperature stabilization needed; • Architecture $1 \times N$ and channel number enlargement by devices; • For system with channel count > 16; • Developed infrastructure needed; • Duplex; • Small polarization mode dispersion values. 	<ul style="list-style-type: none"> • Insertion loss > 6 dB; • Polarization dependent loss ~ 0.2 dB; • Adjacent channel isolation 40 dB; • Channel interval > 6.25 GHz; • Tunable transmission bandwidth and central wavelength; • Low temperature dependence and unstable from mechanical stress; • Architecture 1×1; • Duplex; • Tunable filters are active; • Small dispersion.

Interest in the acquisition of dispersion characteristics for wavelength filters arose in the mid-nineties, and the relevant methods were worked out based on the optical fiber measurement techniques [17, 19, 49]. However, the wavelength filters are selective devices, so in order to characterize them various factors should be taken into account. First of them is

the increasing demand for the dynamic range, since in the domain of the wavelength filter's complex transfer function (where greater dispersion values could be expected) the introduced losses are growing. The second factor is that the dispersion – as function of the wavelength in contrast to the optical fiber case – is a quickly varying parameter, which could be explained by the Kramers-Kronig relations [75]. In turn, the third factor is that the wavelength filters possess a relatively small dispersion as compared with optical fibers.

It is not only the dispersion that affects the wavelength filter's passband needed for separation of the optical signals from the whole WDM system's spectrum; this passband is not always determined by the data transmission speed, since some other factors – such as the influence of temperature, the shifting of the central wavelength of a laser and its aging, as well as the widening of optical signal's spectrum due to the nonlinear optical effects [77]. Therefore, a necessity arises as to the appropriate investigations into the WDM systems with increasing data transmission speed, since the dispersion introduced by wavelength filter can significantly affect the transmitted signal [4, 13, 36]. In the process of working out a wavelength filter especial attention should be given to the shape of the amplitude and phase characteristics. Having preserved the desired phase characteristic ensuring the minimum signal distortion, the search for the appropriate filter amplitude characteristic should be initiated. Taking into account the above-mentioned condition, such an amplitude characteristic is to be close to a rectangle in order to ensure the minimum crosstalk between adjacent channels. At the same time, this condition can create a signal's distortion at increasing data transmission speed, since the level of the induced dispersion is not always minimal [66]. Therefore, it is important to develop a methodology for determination of the effective bandwidth of a wavelength filter and find out the influence of such filter on the optical signal passing through it at a high speed.

For creation of an all-optical communication system it is necessary to search for new ways of wavelength filters' application as well as to work out new-type wavelength filters that would be applicable to the integration with semiconductor devices, which would allow the nanometre sizes to be achieved. One of possible applications would be fully optical conversion of the modulation format with MRR filters, which is required in order to raise the scalability of the future optical communication systems [51, 79, 86]. The RZ-NRZ conversion of signals is a convincing example illustrating the interaction of different future optical communication systems. This is a vital problem, which is to be considered already now for the transport and access optical networks, since it would allow improvement of the efficiency of optical signals' processing thus promoting the total scalability of the future optical communication networks.

Chapter 2

The relevant signals and physical components are describable mathematically by complex functions. The impact of time-domain physical components on the transmitted signal can be estimated through convolution between the function describing a component and the function that characterizes the input signal. Based on the Fourier transform theory, the equivalents for such effects could be estimated in the frequency domain using the Fourier transform from the input signal characteristic and the Fourier transform from the expression describing the physical component [25].

In the work, the acquisition of complex transfer functions is divided into two parts. First, we obtain the amplitude square transfer functions (ATF) and then the phase transfer functions (PTF). Such an order is also connected with accessibility of measuring setups as related to PTF measurements. Owing to successful cooperation of the Institute of Telecommunications with Agilent Technologies Co., in February 2011 the majority (by then) of PTF measurements were taken for the wavelength filters available at the Fiber Optics Transmission System Laboratory.

To find the wavelength filter's ATF two methods could be applied. The main difference between them is the type of the light source. In the former case, a tunable laser source (TLS) is used together with the optical spectrum analyser (OSA). In this case, it is important to synchronize both the devices as well as reach the peak power stability in the measurement range. In such solutions the measuring instruments are usually employed that are mutually controlled using the relevant schemes (see scheme in Fig. 3). In the measurements, an Agilent 86038B tunable laser was used, which was „conjugated” with an optical spectrum analyser. In the following chapters of the work this technique will be referred to as the TLS method.

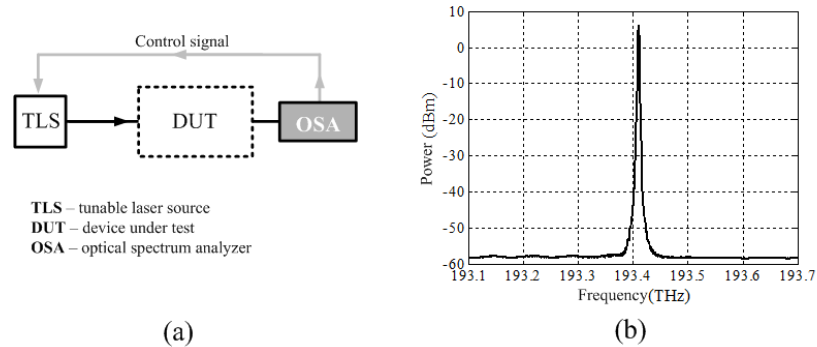


Fig.3. A scheme for measuring the amplitude square transfer function with TLS (a); power spectrum of the continuous TLS (b)

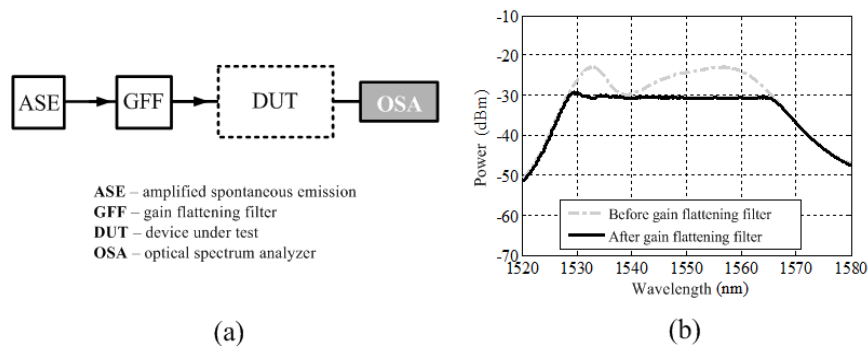


Fig.4. A scheme for measuring the amplitude square transfer function with ASE (a); the power spectra of broadband noise spontaneous emission light source (b)

The main difference of the second method is the light source. In the measuring scheme a source of broadband light is used (for realization see Fig.4). In a particular case no additional control circuit is required for synchronization of the light source with OSA. However, the main limitation of this method is the wavelength range (from 1530 nm to 1565 nm), since the light source in this measuring scheme is executed as that of broadband noise spontaneous emission light (a pumping light source consisting of a laser diode with the central wavelength of 975 nm and a 10 m long EDF). For flattening the power spectrum a gain flattening filter (GFF) and, in addition, ADVANTEST Q8384 OSA are used. In further chapters this method will be named amplified spontaneous emission (ASE) method – the name associated with the light source used.

During the work, the ATF measurements were done for different wavelength filters: TFF, FBG, AWG and DG, which are employed in commercial dense WDM (DWDM) systems. The last of the listed wavelength filters is intended for scientific research due to its being made with tunable wavelength bandwidth (shown below in the description of measurements).

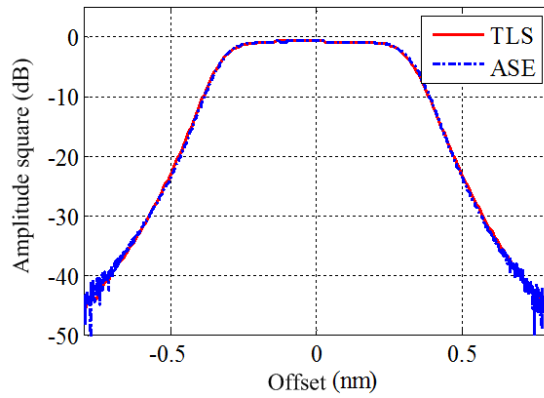


Fig. 5. 100 GHz TFF amplitude square transfer function on logarithmical scale obtained with TLS and ASE methods

Figure 5 shows the amplitude square transfer function for a 100 GHz TFF. The parameters of this filter are: insertion loss 1.2 dB, bandwidth values at the -1 dB, -3 dB and -20 dB levels are, respectively, 68.8 GHz, 81.3 GHz and 118.8 GHz.

To obtain the phase transfer functions, the Agilent 86038B measuring device was used, which allowed for estimation of such wavelength filter's parameters as PTF, group delay (GD) and the induced dispersion as wavelength function. In a particular measuring setup a modulated phase shift (MPS) method was used.

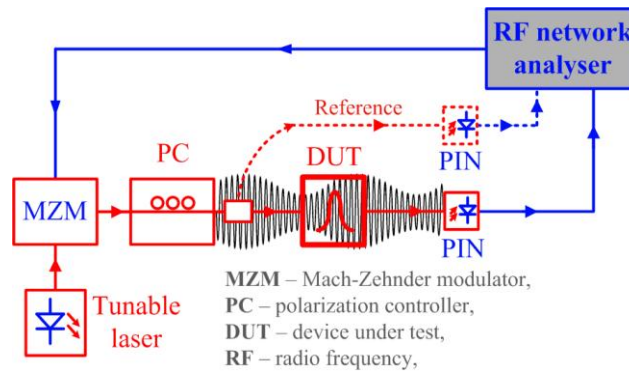


Fig. 6. Measuring scheme for the modulation phase shift method

The modulation phase shift measurement scheme is shown in Fig. 6. Light from a tunable laser is sinusoidally amplitude modulated (typically in the 100 MHz to 1.25 GHz range) in a Mach-Zehnder modulator (MZM). Polarization controller is employed to alter the signal polarization state for differential group delay measurements. After propagating through the device under test (DUT), the transmitted signal is detected by a PIN photodiode. An RF network analyzer is used to provide a modulating signal and to measure the electrical phase difference between input and output signals. This is the most accurate method for measuring the phase characteristics of a real device [1, 18, 66].

The 100 GHz TFF phase transfer function, group delay and dispersion obtained with MPS method are shown in Fig. 7. The group delay changes in the -20 dB bandwidth are 16 ps, while the dispersion equals 0 ps/nm for the central wavelength. The maximum dispersion value in this band is from -111 ps/nm to 141 ps/nm.

The results obtained outside the -20 dB band are noisy, showing the greatest limitations at the wavelength filter measurements. In this case the dynamic range of the measuring technique is sufficient for achieving the required accuracy only inside the passband, which is connected with a high loss inserted by the filter beyond its passband. As a result, the optical signal is attenuated, and the phase value cannot be determined for the network's analyser. A transition region is shown in the results to verify their truthfulness.

The relative group delay is also considered, since its influence on the optical signal propagating through the device is much greater than that of the absolute delay. Besides, it should be taken into account that at decreasing the passband of a wavelength filter the relevant induced dispersion increases, which at higher transmission speeds can lead to degradation of the optical signal. This effect could be even stronger in the case of cascaded filters when the induced dispersion accumulates [66].

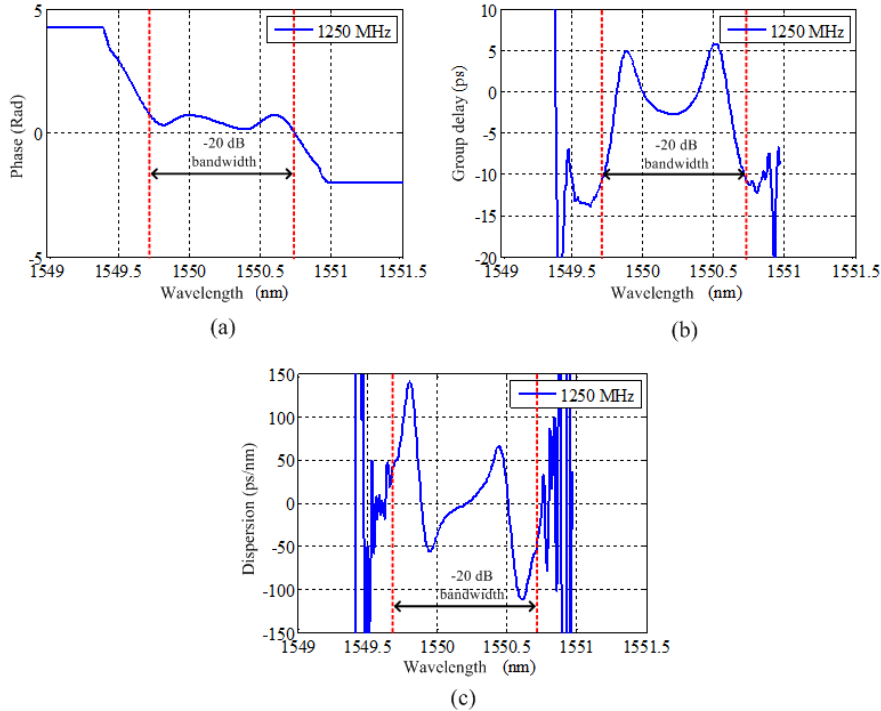


Fig. 7. 100 GHz TFF (a) phase transfer function, (b) group delay and (c) dispersion obtained with MPS method

This chapter describes the complex transfer functions of wavelength filters and the ways of their determination. One of them is to calculate such a function theoretically, and to use it in the cases when the relevant measuring equipment is unavailable. Also, the measuring methods for acquisition of the amplitude square transfer function are considered. Next, a search is done for the solutions related to the acquisition of the phase transfer function using Hilbert's transform of the amplitude square transfer function. This approach has its own limitations – e.g. when real measurement data are used, which quite often are relatively noisy [66]. Therefore, a possibility is considered which involves description of all the filters by definite mathematical functions. This would give some result; however, it should be taken into account that the dispersion induced by this type wavelength filter is highly dependent on its physical realization. Hence, the phase transfer function measurements were preferred, which turned out to be the most precise way of obtaining the dispersion value induced by a wavelength filter's physical realization [66].

Chapter 3

The chapter is structured in three parts: the first part describes a new measuring method worked out for determination of the effective bandwidth of a wavelength filter; the second part is devoted to the developed measuring scheme as well as to the possibility to raise the total spectral efficiency of the system using the same wavelength filtering technologies; in the third part, the most efficient full width at half maximum (FWHM) passbands are determined and recommendations offered as to the conversion of the DPSK optical signal to the Duobinary optical signal using the Lorentzian, Raised Cosine, and Super-Gaussian filters.

As a rule, the manufacturers of wavelength filters use the FWHM criterion. However, this criterion does not allow determination of the maximum admissible shift of the central wavelength of a WDM system's channel from the central wavelength of the filter at the estimation of a signal's distortion. It should be taken into account that at differing transmission speeds such admissible shifts could also be different. Therefore, determination of effective bandwidths is of high importance for the new-generation access systems based on densifying the wavelength-division multiplexing [52, 54, 55, 60, 61]. In such DWDM systems the data transmission speed and the number of channels could be raised gradually. Every flaw in the wavelength filters' parameters might be a source of significant distortion of the transmitted signal's quality. So it is necessary to create such a method for determination of the bandwidth that would take into consideration both the factors – the signal quality achieved and the possible data transmission speed increase [34]. This means the necessity of defining the effective bandwidth. Therefore, in the work the effective bandwidth was defined in whose limits at offset of an optical signal's central wavelength this signal is not degraded, which implies $BER < 10^{-9}$ [57, 58]. For the definition, in the work a block diagram for bandwidth determination (Fig.8) has been developed and patented in Latvia [62].

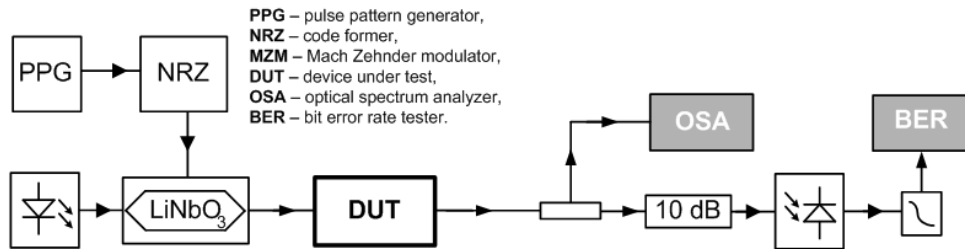


Fig. 8. Effective bandwidth determination measurement setup [62]

Fig. 9 shows the eye diagrams and optical power spectral densities of 10.3125 Gbit/s optical signals after 100 GHz TFF for different laser central wavelength offset values (-0.4 nm, -0.3 nm, 0 nm, 0.3 nm, 0.4 nm). The offset value was changed within TFF device pass-band with 0.1 nm step. This value was chosen to fit DWDM systems' wavelength grid defined in ITU-T G.694.1 recommendation. Other offset values are not shown because greater optical signal amplitude and phase distortions are at the edges of the optical bandpass filter (OBPF). On Fig.9.a and e eye diagrams are shown for -0.4 nm and +0.4 nm offset values and there are mask and signal crossing, which means that the defined BER value is exceeded. From these results the TFF efficient bandwidth is 0.6 nm or 75 GHz [17, 75].

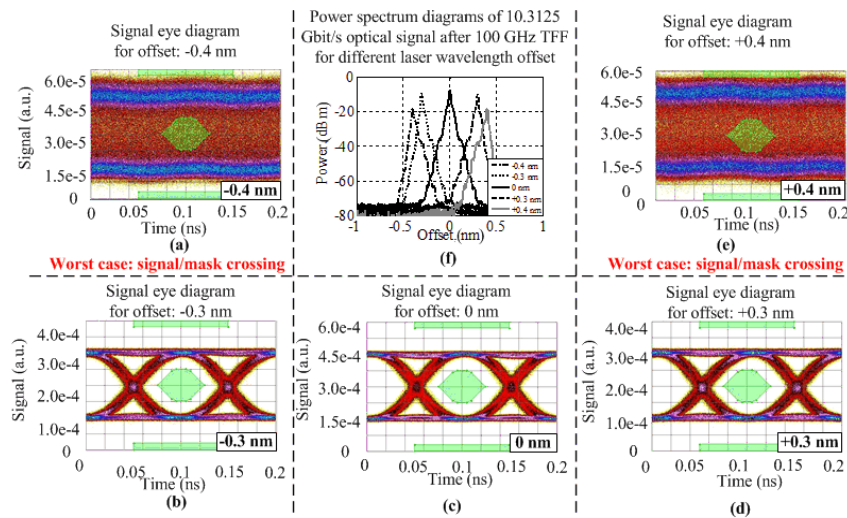


Fig.9. Eye diagrams (a-e) and optical power spectrum (f) of 10.3125 Gbit/s NRZ optical signal after 100 GHz TFF for different CW laser wavelength offsets (shown in inset).

In the case of a TFF wavelength filter – as distinguished from FBG wavelength filters – the effective bandwidth obtained by measurements is independent of the transmission speed. This is due to smaller induced dispersion of the former, which is clearly demonstrated in Table 2 containing the ATF bandwidth values (obtained by ASE method) for the filters under consideration. The tabulated results have been obtained using the practically employed relevant criteria and the developed & patented in Latvia measuring scheme. Comparison of the results obtained allows for the conclusion that the effective bandwidth of the considered TFF wavelength filters is in the range from -1 dB to -3 dB, while in the case of FBG filters it is dependent on the used data transmission speed and decreases at this speed increasing; therefore, the relationship characteristic of the TFF filters is not fulfilled, which is due to a greater value of induced dispersion of FBG wavelength filters [12, 75].

Table 2.

Comparison of bandwidths for wavelength filter in DWDM systems

Filter name	Bandwidth			
	-1 dB level	-3 dB level	-20 dB level	Effective bandwidth
55 GHz FBG	50.0 GHz	55 GHz	75.0 GHz	50 GHz at 2.5 Gbit/s
				25 GHz at 10.3125 Gbit/s
200 GHz TFF	137.5 GHz	200.0 GHz	275.0 GHz	175.0 GHz
100 GHz TFF	68.8 GHz	81.3 GHz	118.8 GHz	75.0 GHz

It is not always possible to determine the least allowed interval between channels in a DWDM system using only the manufacturer-specified wavelength filter parameters. This is indicative of incompletely presented by manufacturer possibilities that could be used for improvement of a WDM system's parameters – e.g. its spectral efficiency [54, 61]. By now different WDM systems have been worked out [7, 14, 50, 88] with the possibility to transmit the information with a definite frequency interval between adjacent channels at a definite data transmission speed for a particular channel. The research on optical communications in the past years was partly directed towards increasing the total capacity of a single optical fiber. The majority of the relevant research works are based on the new modulation techniques suited for definite wavelengths [31, 68]. The proposed approach for increasing the transmission capacity is to reduce the channel spacing of a DWDM system for broadband access to the minimum while keeping the employed wavelength filter technologies [33, 54, 60, 61]. The aim of the relevant invention is to raise the spectral efficiency of a WDM system while applying the existing technologies of wavelength filters. During the work, a measuring block diagram was developed and patented (see Fig. 10) [8].

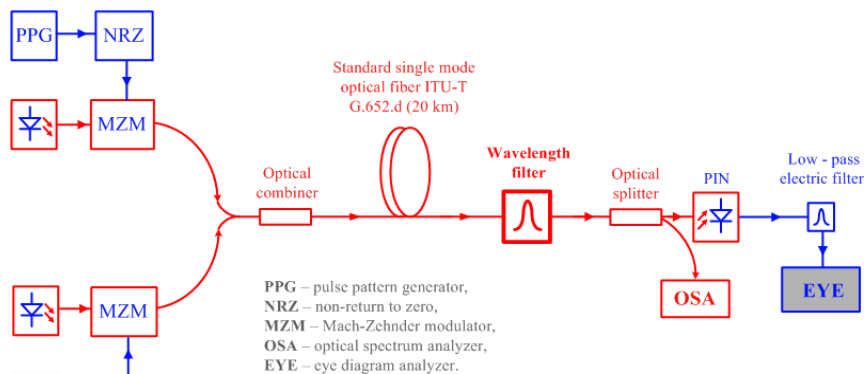


Fig. 10. Scheme for measuring spectral efficiency enlargement [8]

Consider now the results obtained for 200 GHz TFF. Figure 11 shows the eye diagrams and optical power spectral densities of a 10.3125 Gbit/s DWDM system realized with 200 GHz TFF after 20 km of SSMF for different channel intervals from 75 GHz to 175 GHz with 25 GHz (0.2 nm in a wavelength range) step. The step value was chosen to fit DWDM wavelength grid defined in ITU-T G.694.1 recommendation. Both signal's detection in was observed with a 75 GHz channel interval. To reduce undesirable interaction between adjacent signals, the channel interval was increased, which gave lower BER values for the detected signal. As a result, the adjacent channel was suppressed more efficiently, because the steepness of a 200 GHz TFF device is very good and the adjacent channel's isolation is approximately 40 dB. As can be seen from the results (Fig. 11b), a 100 GHz channel interval is sufficient to ensure the appropriate BER value for adequate system's performance. The results for greater channel intervals (125 GHz, 150 GHz and 175 GHz, Figures 10c–e) are also shown to demonstrate DWDM system's stability in the spectral range employed for transmission. Thus, the spectral efficiency of DWDM systems with 200 GHz TFF has risen two times (at 10.3125 Gbit/s transmission speed from 0.05 bit/s/Hz to 0.1 bit/s/Hz).

Using the proposed method: to reduce the frequency interval between the adjacent channels to minimum while applying the same wavelength filters – it is possible to improve the DWDM system's spectral efficiency, which is confirmed by the results obtained.

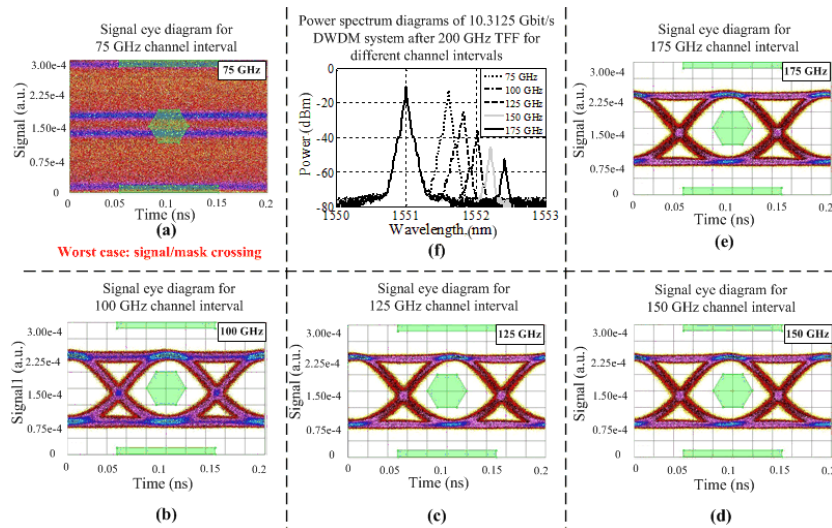


Fig. 11. Eye diagrams (a–e) and optical power spectrum (f) of 10.3125 Gbit/s DWDM system realized with a 200 GHz TFF after 20 km of SSMF for different channel intervals (shown in insets).

Further in the chapter, the complex transfer function is determined which is most suitable for a DWDM system's wavelength filter. Since the decisive factors for this purpose are the data transmission speed and the modulation format, for the research the most widely employed data transmission speeds in the channels of DWDM system and its modulation formats are taken [59, 76].

Travelling through a multiple wavelength filters, the optical signal experiences spectral narrowing due to temperature instability of filtering devices and of central frequency of light sources, which could be the main factor of degradation in future transmission systems [63, 64, 66, 75]. The rate of FWHM band narrowing depends on the shape of the amplitude square transfer function. The fastest FWHM band narrowing at several cascaded wavelength filters is observed for the Lorentzian filter, whereas the slowest – for flat-top filters [59]. In multichannel DWDM systems the above mentioned factors could be the main causes for degradation of transmission signals [38, 53, 88]. Therefore, it was necessary to find out the minimal filter's FWHM bandwidth which ensures appropriate quality of transmitted data signals in compliance with the ITU-T recommendations. Still, the filter bandwidth is not the

exclusive parameter of which we need to be aware. The phase transfer function of wavelength filters is of great importance when we transmit information via DWDM transmission systems at a very high speed in optical channels.

For the research the OptSim 5.0 simulation software was chosen. Three different transfer functions of the optical filter for realization of DWDM system simulation schemes were employed. These functions were chosen because with the Lorentzian optical filter's transfer function we can approximate: Fabry Perrot filters, micro ring resonators; with Raised Cosine: arrayed waveguide grating with a flat top, diffraction gratings, and particular cases of thin film filters and fiber Bragg gratings (with apodization); with Supergaussian: arrayed waveguide gratings with Supergaussian transfer function, and thin film filters with low refraction index modulation [56, 59, 66, 75].

Realization of efficient data transmission at different modulation and coding formats is highly dependent on accurate evaluation of the wavelength filter parameters, because in such modulation and coding formats the power spectrum densities and information distribution are different [44, 76]. Therefore, detailed research into the optical BPF influence on optical signals in DWDM has been carried out. The research is based on the evaluation of such an important system parameter as the Q-factor using simulation techniques incorporated in the OptSim 5.0 simulation software:

$$Q = \frac{m_1 - m_0}{\sigma_1 + \sigma_0}, \quad (1)$$

where m_1 , σ_1 (m_0 , σ_0) are the mean and the standard deviation of the received signal at the sampling instant when a logical "1" ("0") is transmitted. For $Q = 6$ (15.56 dB) the BER value is $\sim 10^{-9}$, and for $Q = 7$ (16.94 dB) $\sim 10^{-12}$ [28].

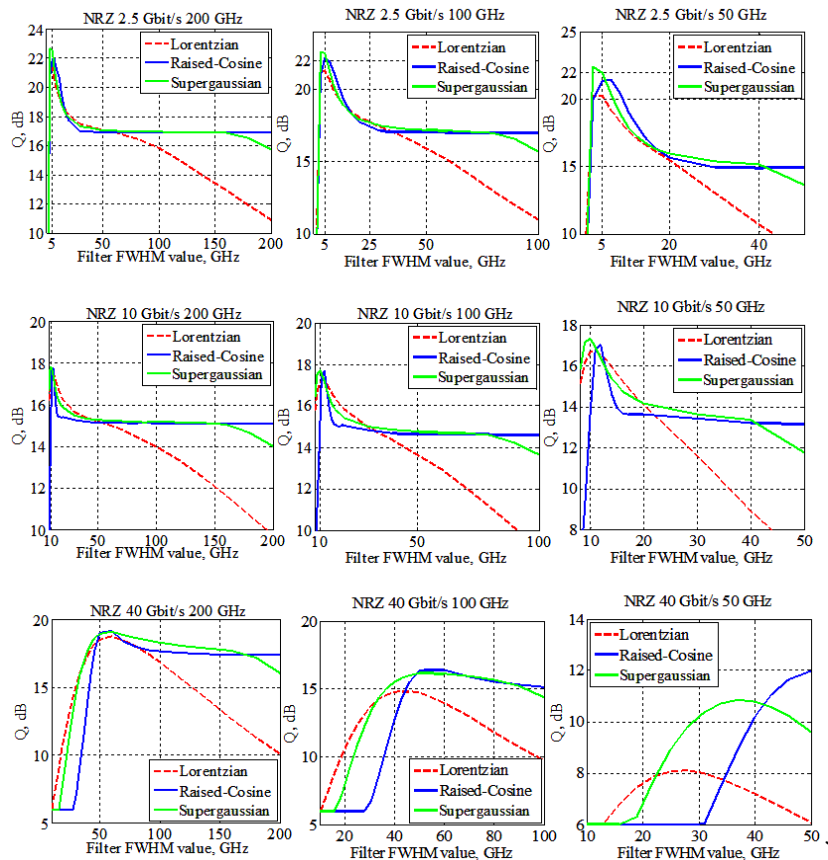


Fig. 12. Q-factor vs. bandwidth for different OBPFs (shown in the inset) of the NRZ-OOK four-channel 2.5/10/40 Gbit/s DWDM system with 50/100/200 GHz channel spacing

In this research the dependences of Q-factor on the FWHM bandwidth of optical band-pass filters with different amplitude transfer functions (Lorentzian, Raised Cosine and Supergaussian) were calculated for various simulation setups: with channel spacings 50/100/200 GHz, data transmission speeds 2.5/10/40 Gbit/s and different modulation formats. The main idea of the research was to find out efficient FWHM bandwidth for different simulation scheme setups. For each modulation format and data transmission speed the length of optical fiber was different by the criterion of realization of reliable data transmission (because increase in the data transmission speed results in greater influence of chromatic dispersion and, therefore, also in nonlinear optical effect), but it was kept the same for all channel intervals.

Figure 12 shows the dependence of Q-factor on the FWHM bandwidth for different optical band-pass filters: Lorentzian, Supergaussian and Raised Cosine for an NRZ-OOK four-channel 2.5/10/40 Gbit/s DWDM system with 50/100/200 GHz channel spacing. It has been shown that speeding-up the data transmission results in a wider spectral density of modulated signal and efficient FWHM bandwidth for different data transmission speeds. This can be explained through the Fourier transformation time and frequency scaling property: compressing a pulse in the time domain will stretch the power spectrum density and vice versa. Besides, a lower channel spacing between adjacent channels results in greater influence of NOEs which reduce the Q-factor for all FWHM bandwidth values.

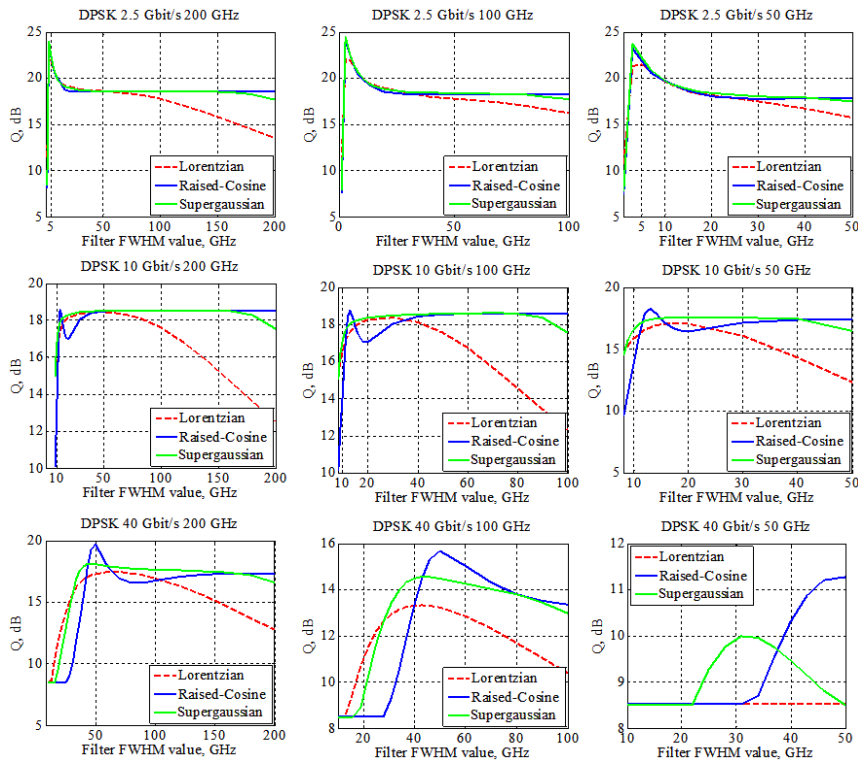


Fig.13. Q-factor vs. bandwidth for different OBPFs (shown in the inset) of the NRZ-DPSK four-channel 2.5/10/40 Gbit/s DWDM system with 50/100/200 GHz channel spacing and balanced detection

The results show that for the NRZ-OOK coded optical signals the FWHM band of efficient filters extends with data transmission speed, and that the best performance is achieved using Supergaussian and Raised Cosine optical BPFs. In the best case the FWHM bandwidth values for 2.5/10/40 Gbit/s data transmission speeds are, respectively, 5 GHz, 10 GHz and 50 GHz. In the case of 40 Gbit/s data transmission speed the 50 GHz channel interval is unsuitable, because Q-factor is here below 15.56 dB (which stands for $BER \approx 10^{-9}$).

To realize reliable transmission for this case the channel interval should be greater – more than 50 GHz.

Figure 13 shows the dependence of Q-factor on the FWHM bandwidth for different optical band-pass filters: Lorentzian, Supergaussian and Raised Cosine, of an NRZ-DPSK four-channel 2.5/10/40 Gbit/s DWDM system with 50/100/200 GHz channel spacing. The greatest data transmission distances for all data transmission speeds are achieved with the NRZ-DPSK modulation format, because of its impressive tolerance for NOEs. The main drawback of this modulation format is its wide spectral density which limits decreasing the channel interval.

The Raised Cosine optical BPF showed the best performance for all data transmission speeds with DPSK-NRZ due to its pass-band shape, which is the closest to the amplitude transfer function of an ideal optical band-pass filter. As distinguished from the previous results, here a more sophisticated design of receiver is used, which is connected with modulation format realization since all the information is recorded in a signal’s phase. As known, it is not always possible to create an especially sophisticated receiver. Therefore, in the work a method is proposed which allows – using narrow-band (Raised Cosine) filtering and a square-law detector – to receive the NRZ-DPSK modulation format.

The results are seen in Fig. 14, where the Q-factor is shown in dependence on the FWHM bandwidth for different wavelength filters of a four-channel NRZ-DPSK 2.5/10/40 Gbit/s DWDM system with a 100 GHz interval between channels, which is realized with a square-law detector. In this case, the phase-to-intensity conversion takes place at decreasing the FWHM bandwidth [21, 43, 85]. The NRZ-DPSK demodulation is a possible cause of lower FWHM bandwidth values, since after the 30 GHz FWHM bandwidth value is reached the signal quality steeply degrades (in the case of Supergaussian filter in Fig. 13) [59]. In turn, the tendency shown in Fig. 14 is quite opposite – the best signal quality in a 40 Gbit/s DWDM system with a 100 GHz inter-channel spacing is at the 24 GHz FWHM bandwidth for Supergaussian filter in the case with square-law detector [11]. Similar results have been obtained (also experimentally) by other authors in whose investigations both Supergaussian and Lorentzian filters were used [21, 43, 85]. In the case of Supergaussian filter the data transmission speed should be multiplied by coefficient 0.6 in order to obtain an appropriate FWHM bandwidth for a DSPK signal’s demodulation. The main contribution of the present work is the NRZ-DPSK demodulation with a Raised-Cosine filter followed by successful detection using a square-law detector.

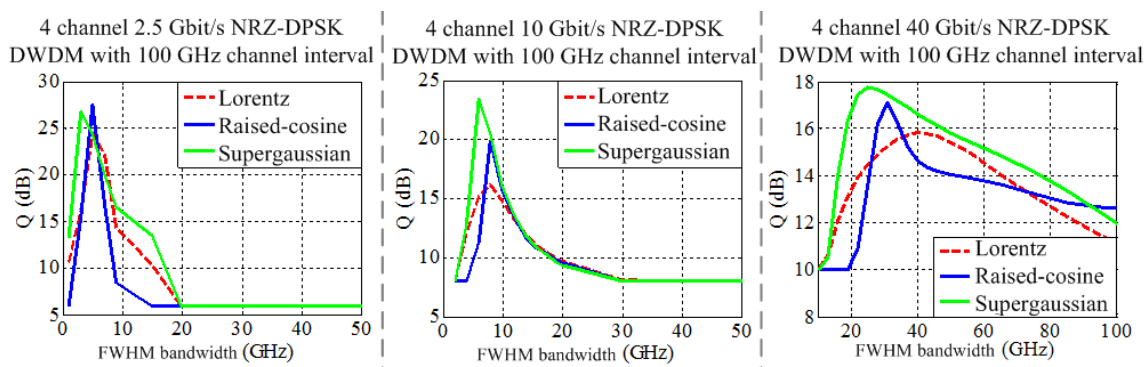


Fig. 14. Q-factor vs. bandwidth for different OBPFs (shown in the inset) of the NRZ-DPSK four-channel 2.5/10/40 Gbit/s DWDM system with 100 GHz channel spacing and direct detection

To verify the trustworthiness of the results obtained, additional experiments have been run for the case of NRZ-OOK modulation format. For this purpose, an additional experimental 2-channel 10 Gbit/s measuring scheme was worked out for variable channel intervals and using a tunable wavelength filter. In the research, an Anritsu “Xtract” DG

wavelength filter was used, which allowed for changing the FWHM bandwidth in the range from 18 GHz to 87.5 GHz. Two FWHM bandwidth values – 18 GHz and 30 GHz – were taken, to make sure that it will be possible to improve the signal quality by narrowing the FWHM band thus reducing the noise level in the receiver. The highest transmission speed was not taken, since in this case the improvement of experimental scheme becomes too expensive.

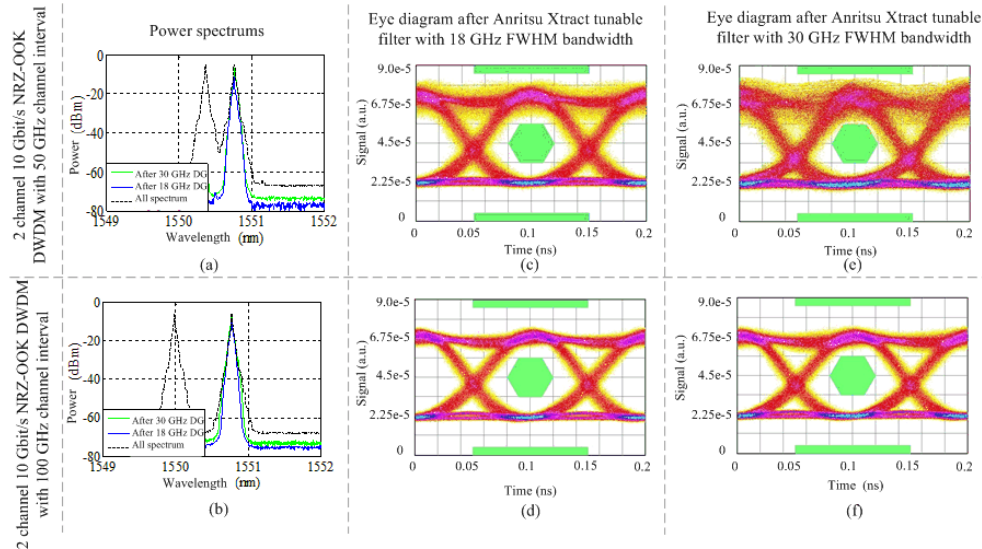


Fig. 15. Experimental 10 Gbit/s DWDM system power spectrum (a, b) worst channel eye diagrams (c-f) and after Anritsu „Xtract” with 18 GHz (c, d) and 30 GHz (e, f) FWHM bandwidth at different channel intervals

Figure 15 shows power spectrums (a, b) of the developed experimental 10 Gbit/s DWDM system and the eye diagrams for the worst channel case (c-f) and after Anritsu “Xtract” at 18 GHz and 30 GHz FWHM bandwidth and 50 GHz and 100 GHz channel spacing. The upper part of the figure presents the results obtained in the case of a 50 GHz channel interval. As could be seen in the diagrams, narrowing the FWHM band it is possible to reduce the ASE noise and improve the signal quality (by raising the Q-factor). From the comparison of the results obtained for different channel intervals it follows that the inter-channel cross-talk and NOEs are decreasing with greater channel intervals, which confirms that these results coincide with those obtained by numerical calculations.

In this chapter, apart from practically applied wavelength filters (whose parameters and capability are estimated using new and patented in Latvia measuring schemes) the general recommendations are given which have been elaborated as to the choice of the complex transfer function for different modulation formats. It is shown that using the Raised-Cosine filter a DPSK signal’s demodulation could be performed, which ensures better resistance against the bandwidth narrowing caused by cascaded filters.

Chapter 4

In Chapter 4, a new-type wavelength filter is considered: the microring resonator (MRR), which so far has not been employed in commercial wavelength-division multiplexing systems. The related research was done during the doctoral practice at the Technical University of Denmark, Photonics Institute, ETDM Laboratory, in cooperation with the scientists from the laboratory of the Wuhan National Optoelectronic and under the supervision of professor Christophe Peucheret. Filters of the type have been extensively studied and described mathematically (see Compendium [67]). Therefore, the primary emphasis in this chapter is placed upon the estimation of MRR limitations and possibilities to

apply these resonators in high-speed optical fiber communication systems; besides, a new solution is proposed for simultaneous conversion of amplitude- and phase-modulated RZ signals to NRZ signals using a single-ring resonator.

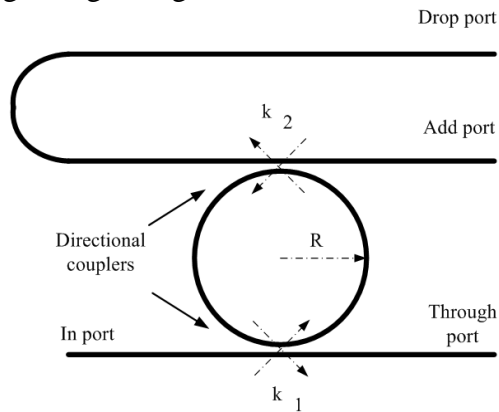


Fig. 16. Structural model of a single ring MRR filter [9, 67]

To describe precisely enough an MRR wavelength filter, mathematical expressions are used that account for the properties of material. Especial attention is paid to the architecture of a single-ring MRR filter, which is explained with simplicity of its design and realization. However, when applying a single MMR filter we should take into account the narrowing of FWHM band when such filters are connected in cascade. First, we will describe a single-ring MRR filter with the following complex transfer functions for the through and drop ports, respectively [67]:

$$E_{through} = \frac{t_1 - t_2 \cdot \alpha \cdot e^{-2 \cdot \pi \cdot i \left(\frac{f - f_0}{FSR} \right)}}{1 - t_1 \cdot t_2 \cdot \alpha \cdot e^{-2 \cdot \pi \cdot i \left(\frac{f - f_0}{FSR} \right)}} \quad (2)$$

$$E_{drop} = \frac{-k_1 \cdot k_2 \cdot \sqrt{\alpha} \cdot e^{-\pi \cdot i \left(\frac{f - f_0}{FSR} \right)}}{1 - t_1 \cdot t_2 \cdot \alpha \cdot e^{-2 \cdot \pi \cdot i \left(\frac{f - f_0}{FSR} \right)}}, \quad (3)$$

where $k_{1,2}$ is a coupling coefficient of the electromagnetic field describing directional couplers (see Fig. 16); $t_{1,2} = 1 - k_{1,2}$ is used to shorten the record, α is an electromagnetic field loss coefficient for one ring; f_0 is the central frequency of MRR filter; $FSR = \frac{c}{2 \cdot \pi \cdot R \cdot n_{eff}}$ is the free spectral range (FSR) or the distance between two central frequencies of the complex transfer function (periodical for these filters); c is the velocity of light in vacuum; R is the MRR radius; and n_{eff} is the effective refractive coefficient [67, 75].

As seen from Fig. 17, the drop port has a Lorentzian filter's shape; in turn, the through port is shaped as a notch filter. These transfer functions are obtained using the Matlab program. Further in the chapter, the limitations and possibilities provided by the transfer functions for the drop and through ports are considered separately. First, the limitations on application of the complex transfer function for the drop port will be discussed.

The relevant investigation was done in order to estimate the degree of an optical signal's degradation at its propagation through multiple cascaded MRR filters. In the investigation, both calculational and experimental methods were used.

Silicon MRRs are versatile devices with promising applications as optical filters or wavelength selective switches [9]. One straightforward use of MRRs is as optical add-drop multiplexers in WDM systems, using MRR structure shown in Fig. 16. Furthermore, thanks to

their compactness, integrability, and compatibility with standard microelectronic fabrication processes, they are essential building blocks for future scalable optical interconnect architectures [70], which have recently been the object of increased research interest. Even though they are designed for high-speed networks or interconnect applications in mind, very few studies have so far considered the impact of MRR filtering on high-speed modulated signals. The system penalty induced by one single or double ring resonator structure on 10-Gbit/s NRZ-OOK signals was first investigated in [39, 46]. Very recently, switching of 10-Gbit/s DPSK signals through a second order silicon microring switch has been demonstrated [81]. Higher order MRRs are used in this context since their wider and flatter passbands prevent the occurrence of phase-to-intensity modulation conversion shown in Fig. 14. The bit-error-ratio (BER) performance of coupled ring resonators has also been given recent consideration for NRZ OOK signals at 10 Gbit/s [24]. However, to constitute a practical solution for MRR-based scalable high-speed interconnect architectures or WDM add-drop nodes, the cascability of the MRRs should be ensured for high bit rate signals, which has not been demonstrated so far. In the present research, the cascability of silicon MRRs used as bandpass filters to their drop port is experimentally investigated for CSRZ-OOK and CSRZ-DPSK signals at 40 Gbit/s [17, 65].

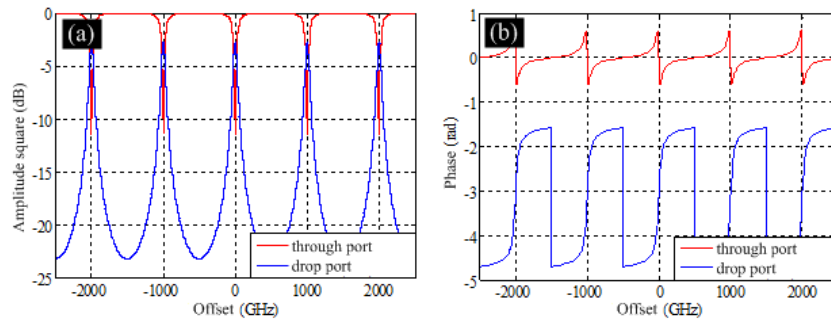


Fig. 17. MRR filter: (a) amplitude square transfer function and (b) phase transfer function for drop and for through ports (FSR = 1000 GHz, $k_{1,2}=0.36$ and $\alpha=0.95$)

The silicon MRR used in the experiment is presented in Fig. 18 a. It was fabricated on a silicon-on-insulator (SOI) wafer with top silicon thickness of 250 nm and buried silicon dioxide of 3 μm . Details of the fabrication process can be found in [20]. The radius of the MRR is 9 μm , with 80-nm coupling gap and 435-nm waveguide width. The input and output waveguides were inversely tapered to 45 nm and covered by polymer. This forms a nano-coupler, which results in ultra-low coupling loss to and from the tapered fibres [20]. Figure 19a shows the measured transfer function at the drop port of the MRR. The measured FSR is 1235 GHz and the Q_{MRR} factor ($Q_{\text{MRR}} = \frac{f_0}{\Delta f_{\text{FWHM}}}$) is 2192, corresponding to a FWHM bandwidth of 88 GHz. The total insertion loss of the device is about 5 dB, and the extinction ratio (ER) of the drop transmission is 20 dB.

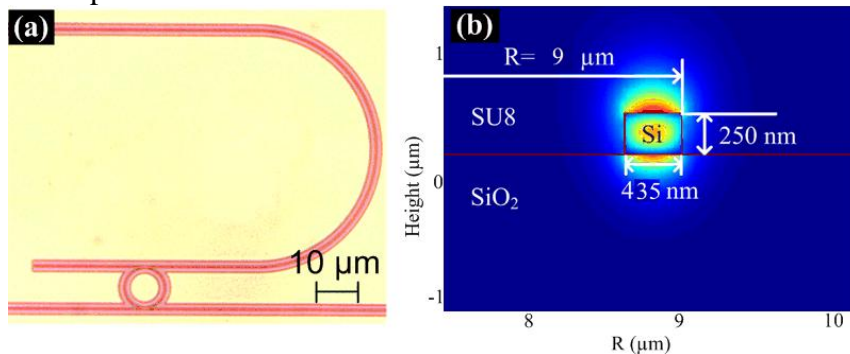


Fig. 18. MRR filter: (a) top view and (b) straight waveguide cross-section

In turn, Fig. 19b shows narrowing of FWHM band in the case when single-ring MRR filters are cascaded. As could be seen, after five cascaded single-ring MRR filters the FWHM bandwidth is 34 GHz, which is estimated to be approximately 60 % smaller as compared with the case of one MRR filter. Such FWHM band narrowing can lead to significant distortions of the transmitted signal.

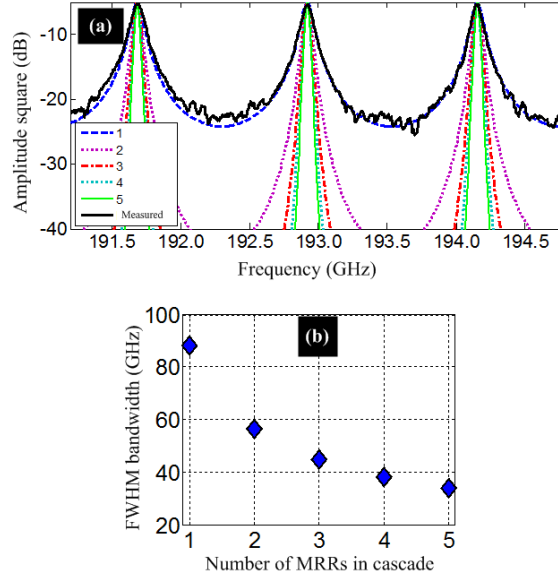


Fig. 19. Realized MRR filter drop port: (a) measured amplitude, its approximation and cascade of approximated function (b) FWHM bandwidth dependence on the number of single ring MRRs in cascade

The experimental recirculating loop setup for investigating the cascability of a single MRR used as drop filter is illustrated in Fig.20. The optical transmitter consists of two LiNbO₃ Mach-Zehnder modulators (MZMs) generating 40-Gbit/s CSRZ-OOK or CSRZ-DPSK signals. The first MZM, driven by a half clock, was used as pulse carver while the second one was driven by a 40-Gbit/s pseudo random binary sequence (PRBS) with a pattern length of $2^{31}-1$. The optical signal was then boosted by an EDFA before being input to the loop. The loop switch consists of two acousto-optic modulators (AOMs). A dispersion compensated span consisting of a 80 km standard single mode fiber and a 13 km dispersion compensating fiber was used to store the data in the loop and enable the recirculations [17, 37].

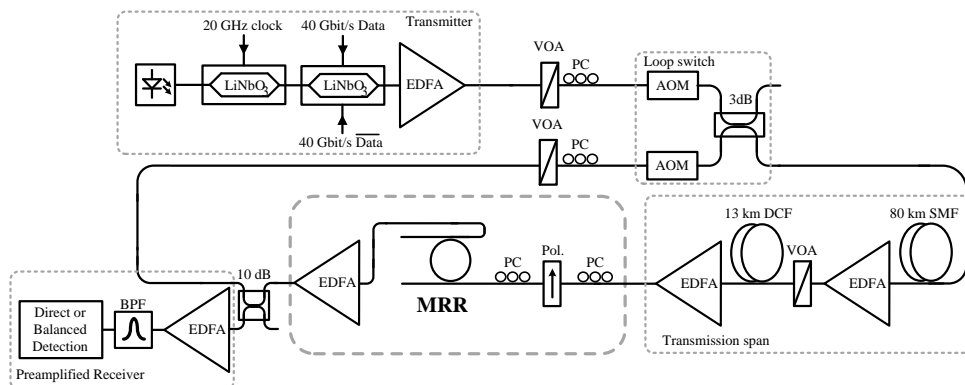


Fig. 20. Recirculating loop setup for MRRs cascability evaluation.

After the transmission span, the optical signal was coupled into the MRR via a tapered fiber and collected again at the drop port by another tapered fiber. An EDFA was used for compensating the insertion and coupling loss of the resonator and loop switch. Data was continuously sent, via a 90/10% coupler, to the receiver. Gating of the BER test-set and the

oscilloscope enabled the characterization of the signal after the last round-trip in the loop. The signal was detected in a preamplified receiver, comprising a 45-GHz photodiode for OOK and a 1-bit fiber delay interferometer followed by a balanced detector, also with 45-GHz bandwidth, for DPSK. Since the MRR is polarization sensitive, it was ensured that the signal at its input was properly polarized for each round trip. This was achieved thanks to a polarizer (Pol.) at its input, and intra- and extra-loop polarization controllers (PCs) enabling to find a stable principal state of polarization for the loop. The experiment with cascaded MRR filters was run using 40 Gbit/s CSRZ-OOK and CSRZ-DPSK modulation formats, the BER value of both the optical signals at the receiver being the primary parameter.

Figure 21 shows the results of BER measurements for the 40-Gbit/s CSRZ-OOK and CSRZ-DPSK signals transmitted through different number of round trips in the loop. The penalty when increasing the number of circulations is induced by bandwidth narrowing, as shown in Fig. 19b, resulting in the waveform degradation and intersymbol interference. The CSRZ-DPSK format can be seen to exhibit larger penalty than CSRZ-OOK [73]. However, dispersion management and noise accumulation are critical at 40 Gbit/s, and some of the measured penalties is actually attributed to the necessary transmission span in the loop. In order to isolate the impact of a MRR on the transmission performance from that of the cascaded transmission spans and loop artifacts, the recirculating loop measurement was repeated with a (broad) 3-nm FWHM TFF replacing the MRR. The bandwidth of the TFF was chosen to be wide enough to ensure that the signal was not affected by any filtering effect even after 5 round trips. A variable optical attenuator (VOA) was inserted in the loop to emulate the insertion loss of the MRR in order to ensure a fair comparison with respect to the noise accumulation.

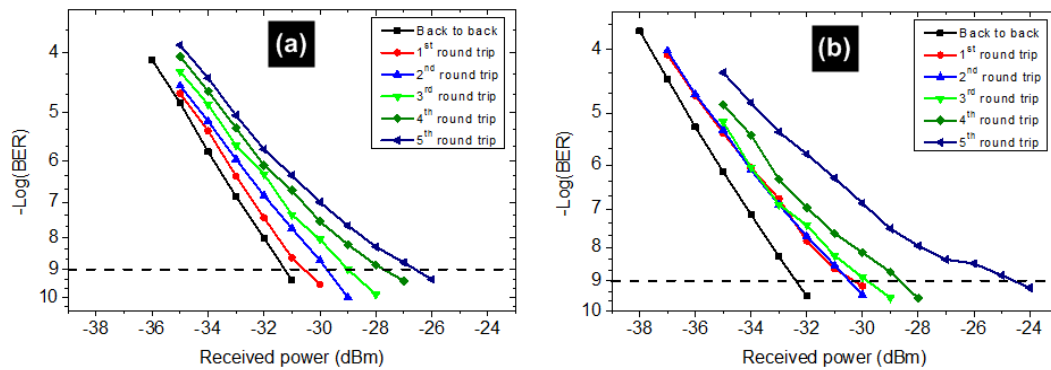


Fig. 21. BER as a function of received power for different number of round trips in the loop and for (a) CSRZ-OOK and (b) CSRZ-DPSK modulation

In order to estimate only the impact of a MRR filter on the transmitted optical signal the BER characteristics were processed assuming $BER=10^{-9}$. As could be seen from Fig. 21, to reach such a BER value the power level should be raised still more. The corresponding power difference is called power penalty. Mathematically, this could be written as:

$$P_{penalty}|_{BER=10^{-9}}(dB) = 10 \cdot \log_{10} \frac{P_1|_{BER=10^{-9}}(mW)}{P_2|_{BER=10^{-9}}(mW)} = P_1|_{BER=10^{-9}}(dBm) - P_2|_{BER=10^{-9}}(dBm), \quad (4)$$

where $P_1|_{BER=10^{-9}}$ is the power required for achieving $BER=10^{-9}$ at the receiver's input, and $P_2|_{BER=10^{-9}}$ is the power required for achieving $BER=10^{-9}$ at the transmitter's output, respectively.

Using equation (4), $P_{penalty}|_{BER=10^{-9}}$ was calculated for BER measurements. Then these values were processed in order to derive only the power penalty due to the impact of a 88 GHz MRR filter. The power penalty values obtained at $BER=10^{-9}$ in dependence on the number of single ring MRR filters in a cascade are displayed in Fig. 22 for 40 Gbit/s

CSRZ-OOK and CSRZ-DPSK optical signals. A power penalty around 1 dB is measured after one single MRR due to its relatively wide (88 GHz) FWHM bandwidth. Similar levels of power penalty are measured for both formats up to 4 cascaded MRRs. After 5 cascaded MRRs, the effective bandwidth of the cascade is reduced to 34 GHz, at which value some DPSK signal demodulation [21] occurs, as can be seen in the corresponding eye diagram (see the inset of Fig. 22). This results in an increased penalty for CSRZ-DPSK compared to CSRZ-OOK.

The cascadability of single silicon MRR and its impact on the performance have experimentally been demonstrated for 40-Gbit/s CSRZ-OOK and CSRZ-DPSK optical signals for the first time. Error-free performance with moderate penalty was measured for both formats after up to 5 cascaded MRRs. The CSRZ-OOK format exhibits a better tolerance to bandwidth narrowing than CSRZ-DPSK, due to the partial DPSK demodulation experienced by the latter format when the effective bandwidth of the MRR cascade is reduced.

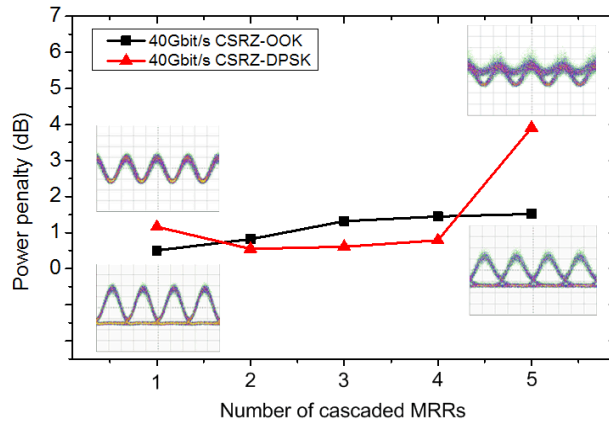


Fig. 22. Power penalty (at BER= 10^{-9}) induced by cascading a single MRR versus number of cascades for CSRZ-OOK and CSRZ-DPSK signals. Insets: eye diagrams after the 1st and 5th round trips.

All-optical conversion between different modulation formats is required to introduce enhanced flexibility in the future optical networks. Format conversion from RZ to NRZ signals is an essential example for interfacing different parts of a future ubiquitous transparent optical network. In the past, significant efforts have been dedicated to on-off keying RZ-to-NRZ conversion using nonlinear optical loop mirrors (NOLMs) [5], active injection locked lasers [15], or SOA [3, 82] with relatively complex configurations. Single and multi-channel format conversions based on simple passive linear filter devices [22, 84, 86] have been demonstrated, however only applied to the on-off keying modulation. On the other hand, because of its improved receiver sensitivity with balanced detection and superior transmission properties [29, 48] differential phase shift keying (DPSK) has received special attention over the past decade. Recently, single [30] and multi-channel [87] RZ-to-NRZ format conversion for DPSK have been experimentally demonstrated using a delay interferometer (DI) with half bit delay. However the dimensions of such devices may remain prohibitively large, which would hinder their potential for integration.

Silicon photonics has received considerable attention lately due to its inherent advantages including compact size and compatibility with microelectronics fabrication processes. Silicon MRRs are versatile ultra-compact devices that have been widely used for all-optical signal processing [42, 78]. Multiple channel RZ-OOK to NRZ-OOK format conversion based on a single silicon MRR has already been successfully demonstrated [22]. In this research, simultaneous RZ-OOK to NRZ-OOK and RZ-DPSK to NRZ-DPSK format conversion at 41.6 Gbit/s based on an optimized silicon microring resonator design was realized. It is shown that the use of an MRR for format conversion is compatible with DPSK

modulation [79]. The effect of the coupling coefficient of the MRR and the bandwidth of the following OBPF on the conversion results were analyzed and then simultaneous conversion for both OOK and DPSK formats at 41.6 Gbit/s was experimentally demonstrated. Clear converted signals eye diagrams and bit-error-rate measurements show the good conversion performance of the scheme [65, 80].

The principle of the format conversion is the linear filtering process at the through port of an MRR [22, 84]. To find appropriate MRR parameters for format conversion a number of simulations were realized in simulation program Matlab. The principle of modulation format conversion is shown in Fig. 23. The simulated eye diagrams of RZ-OOK and RZ-DPSK signals at 41.6 Gbit/s are shown in Figs. 23.a-b. The notch filtering function of the MRR is used to transform the spectrum of an RZ signal to the spectrum of an NRZ signal by suppressing specific spectral components. The spectrum of the input RZ signals (blue) and the transfer function of the MRR with FSR of 83.2 GHz at the through port (green) are shown in Fig. 23c. When the free spectral range (FSR) of the MRR is designed to be twice the signal bit rate, RZ-OOK (respectively DPSK) can be converted to NRZ-OOK (respectively DPSK), at the expense of some amplitude ripple, as shown in Figs. 23d-f, which can be efficiently reduced by an additional optical band-pass filter, as can be seen in Figs. 23g-i. Single ring MRR transmission transfer function is given in formula 2 [67, 83].

The method has already been successfully demonstrated for RZ-OOK to NRZ-OOK conversion [22], but never so far for RZ-DPSK to NRZ-DPSK. Thanks to the frequency periodic filtering characteristic of the MRR, simultaneous conversion of both OOK and DPSK (carried on different wavelength channels) can be realized provided the channel spacing is equal to an integer (≥ 2) multiple of the resonator FSR.

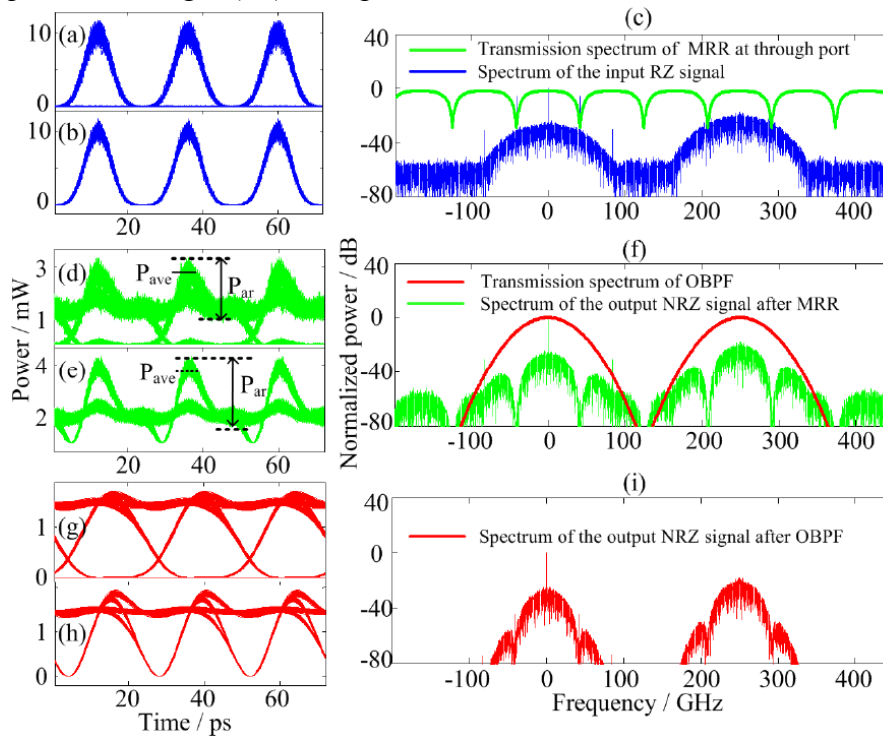


Fig. 23. Principle of the simultaneous format conversion. Eye diagrams of (a) input RZ-OOK and (b) RZ-DPSK at 41.6 Gbit/s. (c) Spectrum of the input RZ signals (blue) and transfer function of the MRR with FSR of 83.2 GHz at the through port (green). Eye diagrams of (d) converted NRZ-OOK and (e) converted NRZ-DPSK after the MRR. (f) Spectrum of the converted NRZ signals after the MRR (green) and transfer function of the OBPF (red). Eye diagrams of (g) converted NRZ-OOK and (h) converted NRZ-DPSK after the OBPF. (i) Spectrum of the output NRZ signals (red) after the OBPF. In these simulations, the power coupling coefficient of the MRR is 0.72 and the FWHM bandwidth of the Gaussian OBPF is 60 GHz.

In order to generalize these observations, we have numerically evaluated the amplitude ripple and the Q value of the converted signal as a function of MRR power coupling coefficient and OBPF bandwidth, as shown in Figs. 24a-d. The amplitude ripple is defined as Par/Pave , where Par is the peak-to-peak power deviation of the high level rail in the converted eye diagram and Pave is its average power, as shown in Figs. 23d-e. Fortunately, the trends of the variations of the ripple and Q value as a function of MRR power coupling coefficient and OBPF bandwidth are found to be similar for OOK and DPSK. For good conversion performance, low ripple and high Q values are required. For a fixed OBPF bandwidth of 125 GHz (~ 1 nm), those quantities have been simulated as a function of the MRR power coupling coefficient. As can be seen in Fig. 24e, when the power coupling coefficient increases, the ripple decreases while the Q value becomes larger. An MRR with power coupling coefficient of 0.9 results in ripple lower than 0.8 and 0.5 and Q values higher than 15 and 30 for the converted NRZ-OOK and DPSK signals, respectively, as shown in Figs. 24f-h.

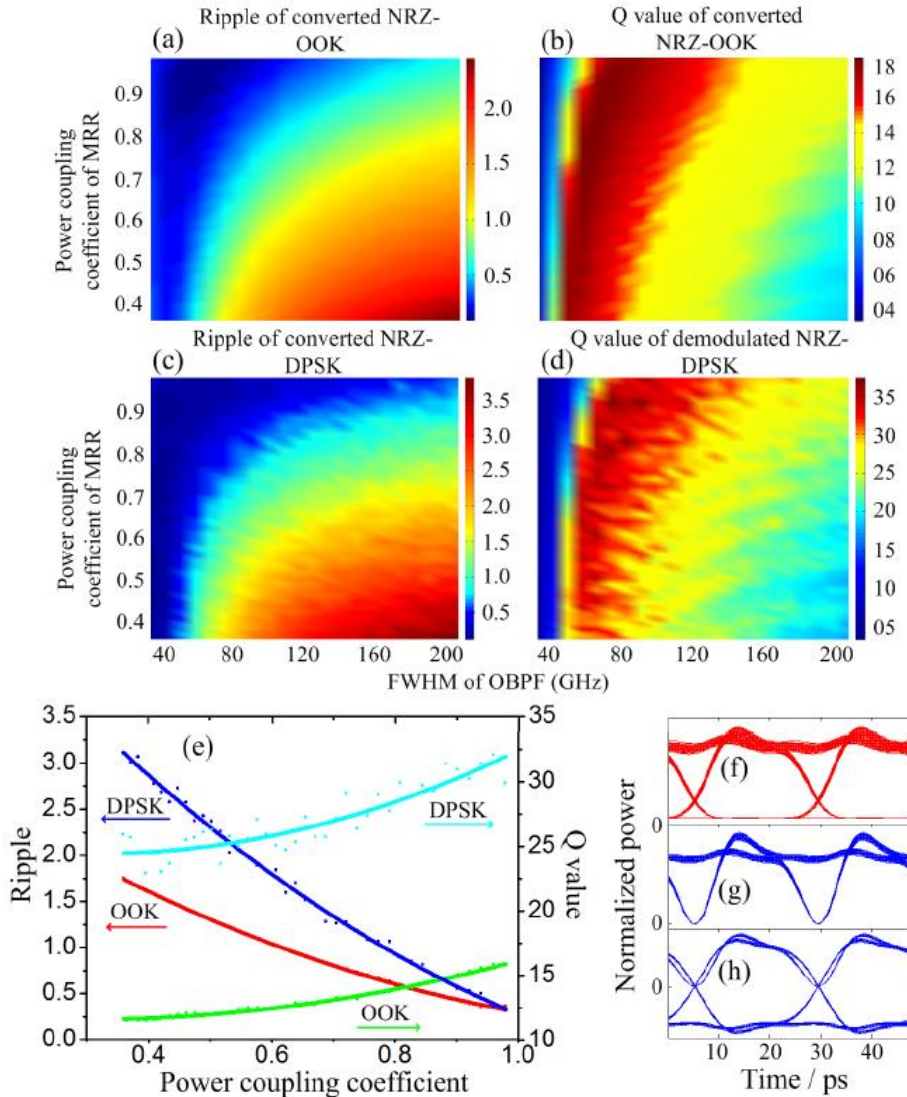


Fig. 24. (a) Calculated amplitude ripple and (b) Q value of the converted NRZ-OOK versus MRR power coupling coefficient and OBPF 3-dB bandwidth at 41.6 Gbit/s. (c) Amplitude ripple of the converted NRZ-DPSK and (d) Q value of the demodulated NRZ-DPSK signal versus MRR power coupling and OBPF 3-dB bandwidth at 41.6 Gbit/s. (e) Amplitude ripple and Q value versus MRR power coupling coefficient for a 1-nm OBPF. Simulated eye diagrams with optimized power coupling of 0.9 for (f) converted NRZ-OOK, (g) converted NRZ-DPSK and (h) demodulated NRZ-DPSK signal after balanced detection with an OBPF of 1 nm.

After having assessed the requirements on the MRR power coupling coefficient for optimum RZ-to-NRZ conversion of both OOK and DPSK formats, we focus on the design and fabrication of a suitable silicon MRR. The 3-D full vectorial film mode matching method (FMM) and coupled mode theory (CMT) [10] are used to design the MRR. An MRR with FSR of 83.2 GHz and high power coupling coefficient is designed. As represented in Fig. 25.a, a silicon-on-insulator (SOI) wafer with a top silicon layer of 250 nm and buried silicon dioxide of 3 mikrometers is used as the platform for MRR fabrication. The width and height of both straight and bend waveguides are 470 nm and 250 nm, respectively. Polymer (SU8-2005) is chosen for the top cladding layer. The waveguide propagation loss is assumed to be 8.2 dB/cm [22].

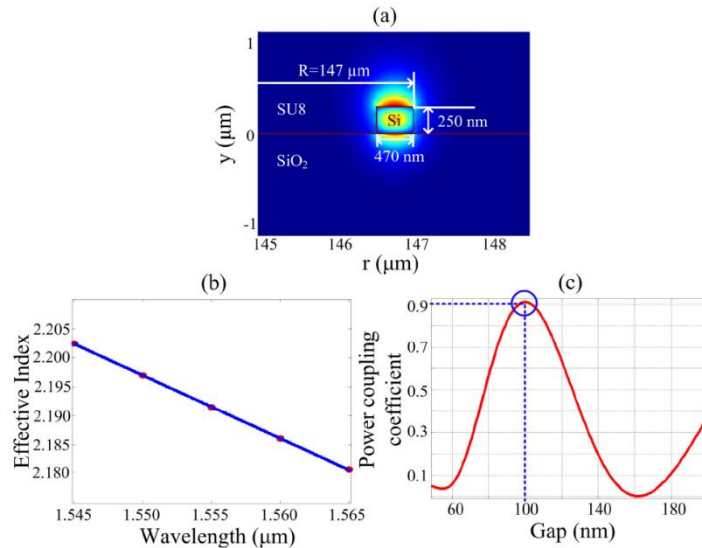


Fig. 25. (a) Cross section and transverse field distribution of the fundamental TM₀ mode of the designed MRR bend rib waveguide. (b) Effective index for the TM₀ mode as a function of wavelength. (c) Calculated coupling coefficient for the TM₀ mode versus the width of the gap between the ring and the straight waveguide.

The structure and mode profile of the silicon waveguides are illustrated in Fig. 4(a). Figure 25.b shows the corresponding effective index for the TM₀ mode as a function of wavelength. The group index is calculated to be 3.9005 at 1550 nm. The radius of the MRR is 147 mikrometers, corresponding to an FSR of 83.2 GHz. Figure 25.c shows the power coupling coefficient versus the dimension of the gap between the ring and the straight waveguide. We can see that a gap of around 100 nm induces a coupling coefficient higher than 0.9, as required for good conversion performance.

The MRR was fabricated on a SOI wafer with top silicon thickness of 250 nm and buried silica of 3 μm. Electron-beam resist ZEP520A was spin-coated on the wafer to create a 110- nm thick masking layer. The MRR structure was defined in the resist layer by electron-beam lithography. Then the patterns were transferred to the top silicon layer by inductively coupled plasma reactive ion etching (ICP-RIE). Due to the linewidth reduction of about 30 nm during the fabrication process, the waveguide width and coupling gap are designed with dimensions of 500 nm and 70 nm, respectively. Figures 5(a)-5(c) show the structure of the device after fabrication. The radius of the MRR is 147 μm with waveguide width of 470 nm and coupling gap of 100 nm, as desired. To decrease the coupling loss to and from the device, a silicon nano-taper, depicted in Fig. 26.c, was adopted. A layer of 3.5 μm polymer (SU8-2005) was spin-coated on the chip. The nano-taper was defined by UV lithography and directly formed by developing. Figure 26.d shows the measured transmission spectrum of the MRR. A low insertion loss of 8 dB is achieved with an FSR of 83 GHz and an extinction ratio (ER) of 25 dB, which corresponds to a power coupling coefficient of 0.9, as designed. The

experimental setup for simultaneous RZ-to-NRZ format conversion of OOK and DPSK is shown in Fig. 27. Continuous wave light at 1549.35 nm is modulated in a Mach-Zehnder modulator pulse carver driven by a 20.8-GHz radio frequency clock and another MZM driven with a 41.6-Gbit/s pseudo-random pattern originating from a bit-pattern generator (BPG), resulting in the generation of a 33% RZ-DPSK signal at 41.6 Gbit/s. Meanwhile, a 33% RZ-OOK signal centered at 1551.36 nm is generated at the same bit rate using another set of two MZMs. The pseudorandom binary sequence (PRBS) length is $2^{31}-1$ for both channels. The OOK and DPSK signals are combined in a 3-dB coupler and then amplified by an EDFA to compensate the insertion loss of the modulators. Before being injected into the MRR, the states of polarization of the signals is adjusted to the TM mode of the MRR with a polarizer (Pol.) sandwiched between two polarization controllers (PCs). The converted NRZ-OOK and NRZ-DPSK signals after the MRR are filtered by an OBPF with 3-dB bandwidth of 1 nm and finally detected in a pre-amplified receiver. A 1-bit fiber DI followed by balanced detection in a pair of 45-GHz photodiodes is used for DPSK detection, while the OOK signal is detected using a single 45-GHz photodiode. The quality of the converted signals is analyzed using an OSA, a 70-GHz sampling oscilloscope and an error analyzer (EA).

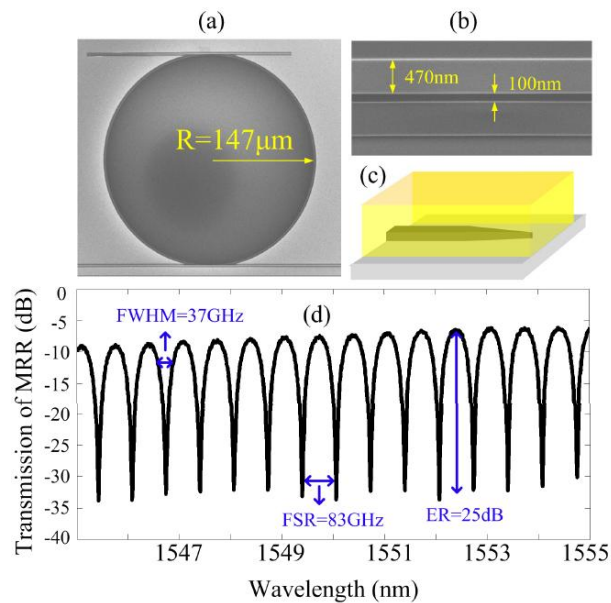


Fig. 26. Scanning electron microscope (SEM) pictures of (a) top view and (b) coupling region of the MRR. (c) Silicon nano taper design. (d) Measured transmission spectrum at the through port of the MRR.

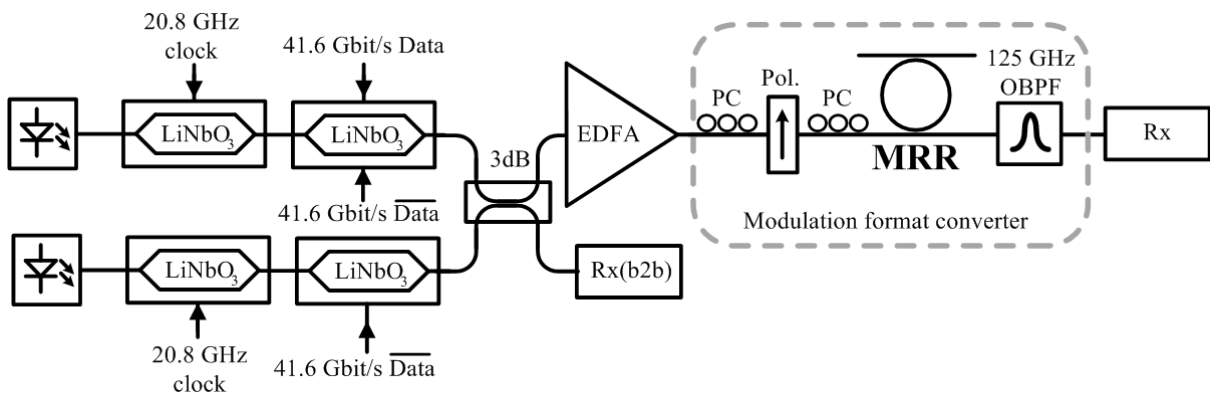


Fig.27. Experimental setup for modulation format conversion.

Firstly the performance of the format conversion is evaluated with single channel operation by switching one of the two channels (OOK or DPSK) off. The central frequency of the input RZ signal is tuned to the center of two notches of the MRR transfer function at the

through port. Figures 28.a and 28.b show the spectra transformation during the format conversion process for OOK and DPSK, respectively. We can see that specific spectral components of both RZ-OOK and RZ-DPSK are suppressed effectively after the MRR and their spectra are successfully transformed to the spectra of NRZ signals. However, the spectra are not significantly affected by the 1-nm OBPF. The same conclusion can be reached by observing the eye diagrams shown in Figs. 28.c-e for OOK and f-h for DPSK. The amplitude ripples of the converted NRZ signals are not reduced significantly using the OBPF. This is because the bandwidth of the OBPF is relatively large while the power coupling coefficient of the MRR is sufficiently high so that the ripples of the converted NRZ signals remain small, in agreement with the numerical analysis of Figs. 24a and c.

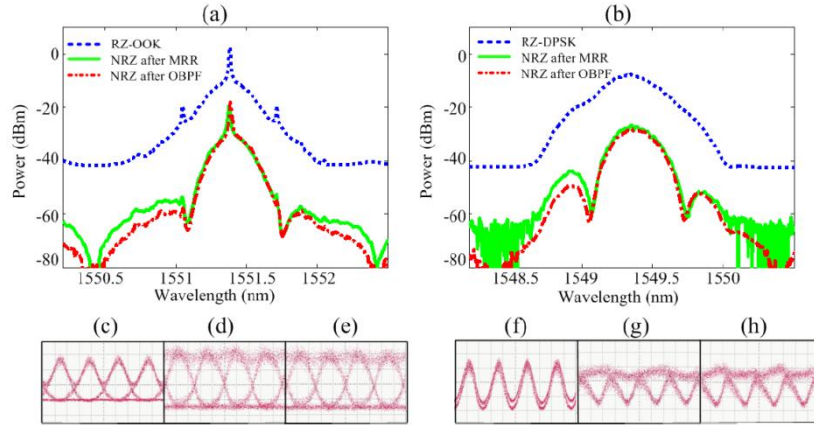


Fig. 28. Measured spectra of the single channel (a) input RZ-OOK, converted NRZ-OOK after MRR, converted NRZ-OOK after OBPF and (b) input RZ-DPSK, converted NRZ-DPSK after MRR, converted NRZ-DPSK after OBPF. The resolution bandwidth is 0.2 nm. Eye diagrams of the single channel (c) input RZ-OOK, (d) converted NRZ-OOK after MRR, (e) converted NRZ-OOK after OBPF, (f) input RZ-DPSK, (g) converted NRZ-DPSK after MRR and (h) converted NRZ-DPSK after OBPF.

For the demonstration of simultaneous format conversion, the OOK and DPSK channels are both turned on. The center frequency of the OBPF is tuned to the OOK channel firstly and then to the DPSK channel prior to detection. Note that a frequency-periodic filter would be used in practice.

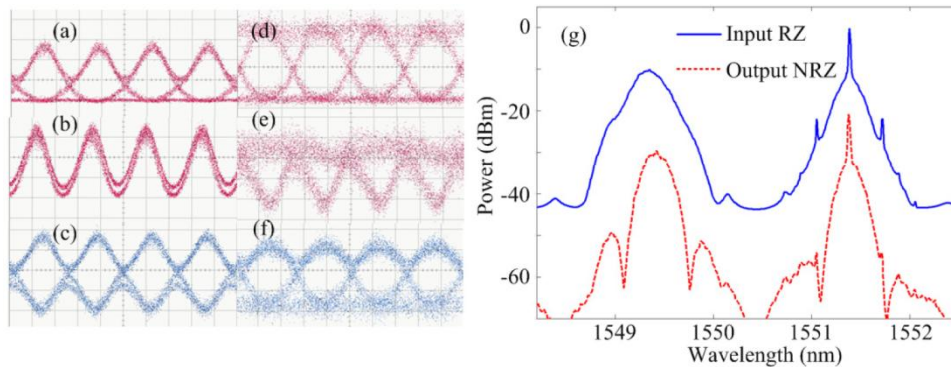


Fig. 29. Measured eye diagrams of (a) input RZ-OOK (single channel), (b) input RZ-DPSK (single channel), (c) demodulated signal of the input RZ-DPSK after balanced detection, (d) converted NRZ-OOK (two-channel), (e) converted NRZ-DPSK (two-channel) and (f) demodulated signal of the converted NRZ-DPSK after balanced detection. (g) Spectra of the two-channel input RZ signals and the converted NRZ signals (resolution bandwidth: 0.2 nm).

Figures 29.a-c show the eye diagrams of the input RZ-OOK and RZDPSK signals and the demodulated RZ-DPSK signal after balanced detection, respectively. Figures 29.d-f show the eye diagrams of the converted NRZ-OOK, NRZ-DPSK and its demodulated signal after balanced detection, respectively. It can be seen that simultaneous format conversion is realized successfully for both channels. The corresponding spectra of the input and output signals after the MRR are shown in Fig. 28.g. The spectra of the two-channel RZ signals are transformed to those of NRZ signals simultaneously. Thanks to the high MRR power coupling coefficient, small ripples are obtained in the converted signals.

Figures 30.a and 30.b show the results of BER measurements for both single channel and simultaneous two-channel format conversion. It can be seen that although there is a hint of error floor, error-free performances are obtained for both OOK and DPSK channels after format conversion (the widely accepted definition of error-free corresponding to BER values below 10^{-9} is adopted here). In the two-channel case, the available power at the receiver was limited to -22 dBm for the converted NRZ-OOK signal, but the BER performance is strictly identical to the single channel case up to the maximum available power, corresponding to a BER of 3.5×10^{-9} . There is nearly no cross talk between the two channels. A small power penalty is measured for DPSK format conversion, while a comparatively larger power penalty of 7 dB, similar to earlier reports [22], is shown for OOK.

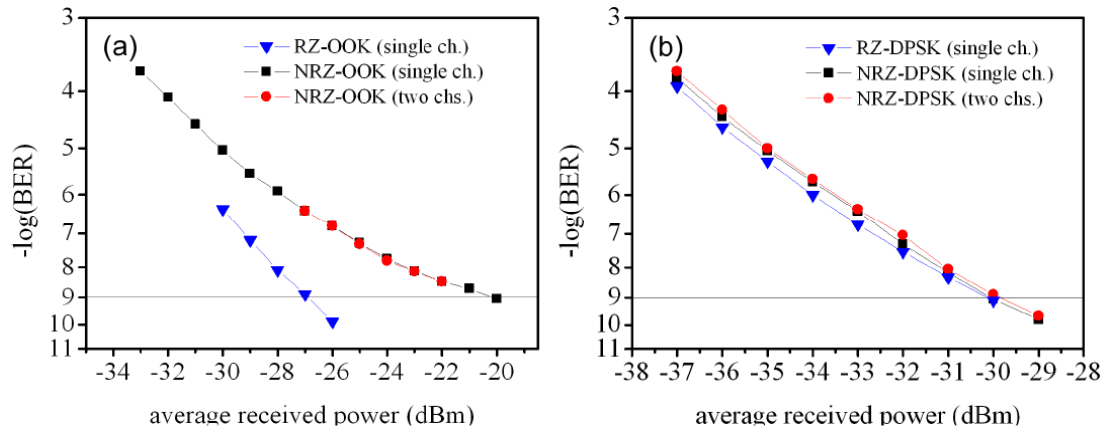


Fig. 30. BER measurements for (a) input RZ-OOK, converted NRZ-OOK for both single and two-channel operations, (b) input RZ-DPSK, converted NRZ- DPSK for both single and twochannel operations.

Simultaneous RZ-to-NRZ format conversion for both OOK and DPSK signals in a well optimized custom-made silicon microring resonator with FSR of 83.2 GHz and power coupling coefficient of 0.9 have been demonstrated. Good converted signal quality is obtained, as attested by eye diagrams and BER measurements at 41.6 Gbit/s.

THE MAIN RESULTS OF THE PROMOTION WORK

The **main results and conclusions of the promotion work** obtained during fulfilment of the tasks defined in Chapter 1 are as follows.

1. The developed algorithm allows for treatment of the obtained – both theoretically and experimentally – of the complex transfer functions of wavelength filters (FBG, TFF, DG, AWG, and MRR) and for creation of user-defined filter models thus supplementing the set of wavelength filter models in simulation programs.
2. A measuring method has been created for determination of the effective bandwidth of the wavelength filters. It is found out that for FBG filters the effective bandwidth is narrowed by half – from 50 GHz in the 2.5 Gbit/s NRZ-OOK case to 25GHz in the 10.3125 Gbit/s NRZ-OOK case, which is associated with a high induced dispersion in the -20 dB band: from -514 ps/nm to 390 ps/nm.

3. For the 100 GHz and 200 GHz TFF devices the effective bandwidths are respectively 75 GHz and 175GHz; besides, the width does not change at the 2.5 Gbit/s and 10.3125 Gbit/s transmission speed, which is explained by a relatively low induced dispersion: for a 100 GHz TFF from -111 ps/nm to 141 ps/nm and for 200 GHz TFF from -49 ps/nm to 45 ps/nm (the values obtained in the -20 dB band).
4. A measuring scheme has been worked out for estimation of possibilities to improve the spectral efficiency of a WDM system. In the case of a 200 GHz TFF device, the spectral efficiency of the 2.5 Gbit/s NRZ-OOK WDM system was raised from 0.05 bit/s/Hz to 0.1 bit/s/Hz, and at the transmission speed of 10.3125 Gbit/s - from 0.0125 bit/s/Hz to 0.025 bit/s/Hz.
5. The most effective wavelength filter's complex transfer function has been found for the separation of an optical signal in dense wavelength division multiplexing systems. The best quality of signals is achievable using Supergaussian and Raised-Cosine filters. In the case of a Raised-Cosine filter the best signal quality was found to be at a lower transmission speed, which is connected with a greater induced group delay as compared with the Supergaussian filter's case.
6. It is shown that with the use of a Raised-Cosine filter it is also possible to perform conversion from the phase modulation format to the intensity modulation format and detect by a square-law detector. Conversion of the type is reported by other authors to be performed using Lorentzian and Supergaussian filters. The proposed solution – i.e. that using a Raised-Cosine filter – as compared with the use of Lorentzian and Supergaussian filters provides better resistance against to the narrowing of passband in the case of cascaded filters. For a 40 Gbit/s NRZ-DPSK optical signals the FWHM bandwidth value of a Raised-Cosine filter should be in the limits from 30 GHz to 40 GHz.
7. A prototype of the micro-ring resonator has been worked out for channel separation and the influence of cascading evaluated on the 40 Gbit/s optical signals with a carrier suppressed return to zero intensity and phase modulation formats. The BER of 10^{-9} was achieved after five cascaded microring resonator filters. The CSRZ-OOK modulation format has been found to be more resistant to the filtering effects as compared with the CSRZ-DPSK modulation format, which could be explained by a partial DPSK demodulation experienced by the latter format when the effective bandwidth of the five-MRR cascade is reduced.
8. A prototype of the micro-ring resonator has also been created for simultaneous RZ to NRZ conversion of 41.6 Gbit/s OOK and DPSK optical signals. The RZ to NRZ conversion of 41.6 Gbit/s DPSK optical signals as well as simultaneous RZ to NRZ conversion of 41.6 Gbit/s OOK and DPSK optical signals have been successfully performed.

Finally, it should be stressed that the results obtained are applicable for improvement of the efficiency and scalability of WDM systems – both commercial and new ones. Apart from that, a new functionality is proposed: the modulation format conversion with a MRR filter, which allows for creation of more flexible new WDM systems. The recommendations worked out in the working process are intended both for improvement of already operating wavelength division multiplexing systems and for implementation of new ones. The recommendations have been practically realized in the framework of a cooperation agreement at J/S „Latvenergo” Co., J/S Ltd „Telia Latvia” Co., and J/S Ltd „TELE2” Co. for investigation and implementation of wavelength division multiplexing systems. Besides, developed and patented in Latvia is a measuring scheme for checking the effective bandwidth of the wavelength filters for raising the efficiency of WDM systems with 2.5 Gbit/s and 10.3125 Gbit/s NRZ-OOK optical signals and a two-channel measuring scheme (also patented in Latvia) for WDM systems with 2.5 Gbit/s and 10.3125 Gbit/s NRZ-OOK optical signals, while retaining the operational wavelength filter.

LITERATURE

1. Agilent Technologies. Agilent 86038B Photonic Dispersion and Loss Analyzer. - Germany: Agilent Technologies Manufacturing GmbH, 2006. – 350.p.
2. Agrawal G. Fiber-Optic Communication Systems. – USA: John Wiley and Sons, 2002. - 561 p.
3. Banchi L., Presi M., D'Errico A., Contestabile G., Ciaramella E. All-optical 10 and 40 Gbit/s RZ-to-NRZ format and wavelength conversion using semiconductor optical amplifiers// J. Lightwave Technol. – 2010. – Vol.28. – 32.-38.p.
4. Becker P.C., Olsson N.A., Simpson J.R., Erbium-Doped Fiber Amplifiers. Fundamentals and Technology. – USA: Academic Press, 1999. - 481.p.
5. Bigo S., Desurvire E., Desruelle B. All-optical RZ-to-NRZ format conversion at 10 Gbit/s with nonlinear optical loop mirror// Electron. Lett. – 1994. – Vol.30. – 1868.-1869.p.
6. Binh N. Photonic Signal Processing. Techniques and Applications. – USA: CRC Press, 2008. - 382.p.
7. Bobrovs V., Ivanovs Ģ. Investigation of Minimal Channel Spacing in HDWDM Systems// Electronics and Electrical Engineering, - 2009. – Vol. 4(92) – 53.-56.p.
8. Bobrovs V., **Ozoliņš O.**, Ivanovs Ģ., Poriņš J. Viļņgarumdales blīvēšanas sakaru sistēma ar šaurjoslas filtru// Latvijas patents. - 20.02.2010. - LV-14107. – 1.-8.p.
9. Bogaerts W., De Heyn P., Van Vaerenbergh T., De Vos K., Selvaraja S. K., Claes T., Dumon P., Bienstman P., Van Thourhout D., Baets R. Silicon microring resonators// Laser Photonics Rev. – 2012. - Vol.6, - 47.-73.p.
10. Cai X.L., Huang D.X., Zhang X.L. Numerical analysis of polarization splitter based on vertically coupled microring resonator// Opt. Exp. – 2006. – Vol.14. – 11304.-11311.p.
11. Calabretta N., Presi M., Contestabile G., Ghiggino P., Ciaramella E., Cavaliere F., Proietti R. Optical PON Network Using Passive DPSK Demodulation// US Patent Application Publication. - 09/23/2010. - US 2010/0239258 A1. – 1.-9.p.
12. Caspar C., Foisel H.M., Helmolt C.V., Strebel B., Sugaya Y. Comparison of cascading performance of different types of commercially available wavelength (de)multiplexers //Electron. Lett. – 1997. – Vol.33. – 1624.-1626.p.
13. Cerutti I., Fumagalli A., Rajagopalan R., Barros R., Rossi S. Impact of Polarization Mode Dispersion in Multi-Hop and Multi-Rate WDM Rings// Photonic Network Communications. - 2003. - Vol.5. - 259.-271.p.
14. Chen D.Z., Xia T.J., Wellbrock G., Mamyshev P., Penticost S., Grosso G., Puc A., Perrier P., Fevrier H. New Field Trial Distance Record of 3040 km on Wide Reach WDM With 10 and 40 Gb/s Transmission Including OC-768 Traffic Without Regeneration// J. Lightwave Technol. – 2007. – Vol.25. – 28.-37.p.
15. Chow C.W., Wong C.S., Tsang H.K. All-optical RZ to NRZ data format and wavelength conversion using an injection locked laser// Opt. Commun. – 2003. – Vol.223. – 309.-313.p.
16. Cisco Systems. Cisco Visual Networking Index: Forecast and Methodology 2011–2016// White paper. – 2012. – Vol.1. – 1.-16.p.
17. Cohen L.G. Comparison of single-mode fiber dispersion measurement techniques //J. Lightwave Technol. – 1985. – Vol.3. – 958.-966.p.
18. Dennis T., Williams P.A. Achieving High Absolute Accuracy for Group-Delay Measurements Using the Modulation Phase-Shift Technique// J. Lightwave Technol. – 2005. Vol.23(11). - 3748.-3754.p.
19. Derickson D. Fiber Optic Test and Measurement. – USA: Prentice Hall, 1998. – 642.p.
20. Ding Y., Hu H., Galili M., Xu J., Liu L., Pu M., Hansen Mulvad H.C., Katsuo Oxenløwe L., Peucheret C., Jeppesen P., Zhang X., Huang D., Ou H. Generation of a

- 640 Gbit/s NRZ OTDM signal using a silicon microring resonator// *Opt. Express.* – 2011. – Vol.19. – 6471.-6477.p.
21. Ding Y., Xu J., Peucheret C., Pu M., Liu L., Seoane J., Ou H., Zhang X., Huang D. Multi-Channel 40 Gbit/s NRZ-DPSK Demodulation Using a Single Silicon Microring Resonator// *J. Lightwave Technol.* – 2011. – Vol.29. – 677.-684.p.
 22. Ding Y.H., Peucheret C., Pu M.H., Zsigri B., Seoane J., Liu L., Xu J., Ou H.Y., Zhang X.L., Huang D.X. Multi-channel WDM RZ-to-NRZ format conversion at 50 Gbit/s based on single silicon microring resonator// *Opt. Express.* – 2010. – Vol.18. – 21121.-21130.p.
 23. Dutta A.K., Dutta N.K., Fujiwara M. *WDM Technologies: Passive Optical Components.* – USA: Academic Press. 2003. – 551.p.
 24. Ferrari C., Canciamilla A., Morichetti F., Sorel M., Melloni A. “Penalty-free transmission in a silicon coupled resonator optical waveguide over the full C-band// *Opt. Lett.* - 2011. – Vol.36. – 3948.-3950.p.
 25. Folland G. B. *The Fourier analysis and its applications.* – USA: Wadsworth, 1992. - 441.p.
 26. G. Lenz, B. J. Eggleton, C.K. Madsen, C. R. Giles, and G.Nykolak Optimal dispersion of optical filters for WDM systems // *IEEE Photon. Technol. Lett.* – 1998 – Vol.10. – 567.-569.p.
 27. Ghatak A., Thyagarajan K. *Introduction to fiber optics.* – UK: Cambridge University Press. 2008. - 565.p.
 28. Giles C. R., Desurvire E. Propagation of signal and noise in concatenated erbium-doped fiber amplifiers// *IEEE Journal of Lightwave Technology.* - 1991. - Vol.9. - 271.-283.p.
 29. Gnauck A.H., Chandrasekhar S., Leuthold J., Stulz L. Demonstration of 42.7 Gb/s DPSK receiver with 45 photons/bit sensitivity// *IEEE Photon. Technol. Lett.* – 2003. – Vol.15. – 99.-101.p.
 30. Groumas P., Katopodis V., Kouloumentas C., Bougioukos M., Avramopoulos H. All-optical RZ-to-NRZ conversion of advanced modulated signals// *IEEE Photon. Technol. Lett.* – 2012. – Vol.24. – 179.-181.p.
 31. Hansen Mulvad H.C., Galili M., Oxenløwe L.K., Hu H., Clausen A., Jensen J.B., Peucheret C., Jeppesen P. Demonstration of 5.1 Tbit/s data capacity on a single-wavelength channel// *Optics Express.* - 2010. – Vol.18(2). – 1438.-1443.p.
 32. Hecht J. Recycled Fiber Optics, How Old Ideas Drove New Technology// *Optics and Photonics News.* – 2012. - Vol.23(2). – 22.-29.p.
 33. Ivanovs Ģ., Bobrovs V., **Ozoliņš O.**, Poriņš J. Realization of HDWDM Transmission System // *International Journal of Physical Sciences.* - 5. (2010) -452.-458.p.
 34. Khrais N.N., Elrefaie A.F., Wagner R.E. Performance degradations of WDM systems due to laser and optical filter misalignments// *Electronics Letters.* – 1995. - Vol.31(5). – 1179.-1180.p.
 35. Khrais N.N., Shehadeh F., Chiao J.C., Vodhanel R.S., Wagner R.E. Multiplexer eye-closure penalties for 10 Gb/s signals in WDM networks // *Optical Fiber Communications Conference Proceedings.* - San Jose, California, USA, 1996. 1.-2.p.
 36. Kuznetsov M., Froberg N.M., Henion S.R., Rauschenbach K.A. Power Penalty for Optical Signals Due to Dispersion Slope in WDM Filter Cascades// *IEEE Photonics Technology Letters.* – 1999. - Vol.11(11). – 1411.-1413.p.
 37. Lali-Dastjerdi Z., **Ozoliņš O.**, An Y., Cristofori V., Da Ros F., Kang N., Hu H., Hansen Mulvad H., Rottwitt K., Galili M., Peucheret C. Demonstration of Cascaded In-Line Single-Pump Fiber Optical Parametric Amplifiers in Recirculating Loop Transmission // *European Conference on Optical Communications (ECOC) 2012: Proceedings, Nīderlande, Amsterdam, 16.-20. septembris, 2012.* - 1.-3.p.
 38. Laude J.P. *DWDM Fundamentals, Components, and Applications* - London: Artech House, 2002. – 282.p.

39. Lee B.G., Small B.A., Bergman K., Xu Q., Lipson M. Transmission of high-data-rate optical signals through a micrometer-scale silicon ring resonator// *Opt. Lett.* – 2006. – Vol.31. – 2701.-2703.p.
40. Lenz G., Eggleton B.J., Giles C.R., Madsen C.K., Slusher R.E. Dispersive properties of optical filters for WDM systems // *IEEE J. Quantum Electron.* – 1998. – Vol.34. – 1390.–1402.p.
41. Lenz G., Nykolak G., Eggleton B.J. Dispersion Of Optical Filters In WDM Systems: Theory And Experiment// *European Conference on Optical Communications Proceedings.* - Madrid, Spain, 1998. – 271.-272.p.
42. Liu F.F., Wang T., Qiang L., Ye T., Zhang Z.Y., Qiu M., Su Y.K. Compact optical temporal differentiator based on silicon microring resonator// *Opt. Express.* – 2008. – Vol.16. – 15880.–15886.p.
43. Lyubomirsky I., Chien C.C. DPSK Demodulator Based on Optical Discriminator Filter// *Photonics Technology Letters.* – 2005. – Vol.17(2). – 492.–494.p.
44. Lyubomirsky, I. Advanced modulation Formats for Ultra-Dense Wavelength Division Multiplexing// *White paper.* - 2007. – Vol.1. – 1.–14.p.
45. Ļašuks I., Ščemeļevs A., **Ozoliņš O.** Investigation of Spectrum-Sliced WDM System // *Electronics and Electrical Engineering.* - 5. (2008) 45.-48.p.
46. Melloni A., Martinelli M, Cusmai G., Siano R. Experimental evaluation of ring resonator filters impact on the bit error rate in non-return to zero transmission systems// *Opt. Commun.* – 2004. –Vol.234. – 211.-216.p.
47. Mitra P.P., Stark J.B. Nonlinear limits to the information capacity of optical fibre communications// *Letters to Nature.* – 2001. - Vol.411. – 1027.–1030.p.
48. Mizuoichi T., Ishida K., Kobayashi T., Abe J., Kinjo K., Motoshima K., Kasahara K. A comparative study of DPSK and OOK WDM transmission over transoceanic distances and their performance degradations due to nonlinear phase noise// *J. Lightwave Technol.* – 2003. – Vol.21. – 1933.–1943.p.
49. Niemi T., Uusimaa M., Ludvigsen H. Limitations of the phase shift method in measuring dense group delay ripple in fiber Bragg gratings// *IEEE Photonics Technology Letters.* 2001. - Vol.13(12) – 1334.-1336.p.
50. Oda S., Tanimura T., Cao Y., Hoshida T., Akiyama Y., Nakashima H., Ohshima C., Sone K., Aoki Y., Yan M., Tao Z., Rasmussen J.C., Yamamoto Y., Sasaki T., 80×224 Gb/s Unrepeated Transmission over 240 km of Large-Aeff Pure Silica Core Fibre without Remote Optical Pre-amplifier// *European Conference on Optical Communications Proceedings.* – Geneva, Switzerland, 2011. – 1.-3.p.
51. **Ozoliņš O.**, An Y., Lali-Dastjerdi Z., Ding Y., Bobrovs V., Ivanovs Ģ., Peucheret C. Cascadability of Silicon Microring Resonators for 40-Gbit/s OOK and DPSK Optical Signals// *Asia Communications and Photonics Conference Proceedings.* – Guangzhou (Canton), China, 2012. – 1.-3.p.
52. **Ozoliņš O.**, Ivanovs Ģ. Realization of Optimal FBG Band-Pass Filters for High Speed HDWDM // *Electronics and Electrical Engineering.* - 4. (2009) 41.-44. p.
53. **Ozoliņš O.**, Bobrovs V., Ivanovs Ģ. DWDM Transmission Based on the Thin-Film Filter Technology// *Latvian Journal of Physics and Technical Sciences.* – 2011. – Vol.3. – 55.-65.p.
54. **Ozoliņš O.**, Bobrovs V., Ivanovs Ģ. DWDM-Direct Access System Based on the Fiber Bragg Grating Technology// *8th International Symposium on Communication Systems, Networks and Digital Signal Processing Proceedings.* - Poland, Poznan, 2012. - 1.-4.p.
55. **Ozoliņš O.**, Bobrovs V., Ivanovs Ģ. DWDM-Direct System with FBG Technology for New-Generation Optical Access// *IEEE Swedish Communication Technologies Workshop Proceedings.* - Sweden, Stockholm, 2011. - 10.-10.p.
56. **Ozoliņš O.**, Ivanovs Ģ. Estimation of DWDM Transmission for Broadband Access with FBG Technology // *Electronics and Electrical Engineering.* - 5. (2011) 11.-14. p.

57. **Ozoliņš O.**, Bobrovs V., Ivanovs Ģ. Efficient Bandwidth Measurements of Thin Film Filters for Next-Generation Optical Access// PGNNet2011 Conference Proceedings. – Great Britain, Liverpool, 2011. - 275.-280.p.
58. **Ozoliņš O.**, Bobrovs V., Ivanovs Ģ. Efficient Bandwidth of 50 GHz Fiber Bragg Grating for New-Generation Optical Access// 19th IEEE Telecommunications Forum. - Serbia, Belgrade, 2011. - 816.-819.p.
59. **Ozoliņš O.**, Bobrovs V., Ivanovs Ģ. Efficient Wavelength Filters for DWDM Systems// Latvian Journal of Physics and Technical Sciences. – 2010. – Vol.6. - 47.-58.p.
60. **Ozoliņš O.**, Bobrovs V., Ivanovs Ģ. Evaluation of Optical Filters for DWDM-Direct in Next Generation Optical Access // Developments in Optics and Communications 2011 Book of Abstracts, Latvia, Riga, April 28-30, 2011. - 42.-43.p.
61. **Ozoliņš O.**, Bobrovs V., Ivanovs Ģ., Lasuks I. New-Generation Optical Access System Based on the Thin Film Filter Technology// International Journal of the Physical Sciences. – 2011. – Vol.6(35). - 7926.-7934.p.
62. **Ozoliņš O.**, Bobrovs V., Spolītis S., Udaļcovs A., Ivanovs Ģ. Viļņa garuma filtru efektīvās caurlaides joslas mērījumu shēma// Latvijas patenta pieteikums. - 31.05.2012. - P-12-90. 1.-8.p.
63. **Ozoliņš O.**, Ivanovs Ģ. New Generation Access System Based On DWDM-Direct With 55 GHz Fiber Bragg Grating // Developments in Optics and Communications 2012: Book of Abstracts, Latvija, Rīga, 12.-14. aprīlis, 2012. - 80.-81.p.
64. **Ozoliņš O.**, Ivanovs Ģ. Evaluation of Band-Pass Filters Influence on NRZ Signal in HDWDM Systems // Electronics and Electrical Engineering. - 4. (2010) 65.-68.p.
65. Peucheret C., Ding Y., Ou H., Xiong M., An Y., Lorences Riesgo A., Xu J., **Ozoliņš O.**, Hu H., Galili M., Huang B., Pu M., Ji H., Seoane J., Liu L., Zhang X. **[Invited]** Linear Signal Processing Using Silicon Micro-Ring Resonators //International Photonics and OptoElectronics Meetings (POEM 2012-IONT): Proceedings, Ķīna, Wuhan, 1.-2. novembris, 2012. - 1.-1.p.
66. Peucheret C., Palle J. Fibre and component induced limitations in high capacity optical networks. Doctoral thesis. – Denmark: Technical University of Denmark, 2004. - 274.p.
67. Rabus D.G. Integrated Ring Resonators: The Compendium. – USA:Springer, 2007. – 272.p.
68. Richter T. PalushaniE., Schmidt-Langhorst C., Nolle M., Ludwig R., Schubert C., Single Wavelength Channel 10.2 Tb/s TDM-Data Capacity using 16-QAM and Coherent Detection// National Fiber Optic Engineers Conference proceedings. - Los Angeles, California, USA, 2011. – 1.-3.p.
69. Sano A., Masuda H., Kobayashi T., Fujiwara M., Horikoshi, K., Yoshida, E., Miyamoto, Y., Matsui M., Mizoguchi M., Yamazaki H., Sakamaki Y., Ishii, H. 69.1-Tb/s (432 × 171-Gb/s) C- and extended L-band transmission over 240 km Using PDM-16-QAM modulation and digital coherent detection// Optical Fiber Communication Conference Proceedings. - San Diego, CA, 2010. – 1.-3.p.
70. Siracusa D., Linzalata V., Maier G., Pattavina A., Ye Y., Chen M. Hybrid architecture for optical interconnection based on micro ring resonators// Global Telecommunications Conference Proceedings. – Huston, Texas, USA, 2011. – 1.-5.p.
71. Sivarajan R., Ramaswami K.N. Optical Networks: A Practical Perspective. – USA: Elsevier. 2010. – 893.p.
72. Takara H., Sano A., Kobayashi T., Kubota H., Kawakami H., Matsuura A., Miyamoto Y., Abe Y., Ono H., Shikama K., Goto Y., Tsujikawa K., Sasaki Y., Ishida I., Takenaga K., Matsuo S., Saitoh K., Koshiba M., and Morioka T. 1.01-Pb/s (12 SDM/222 WDM/456 Gb/s) Crosstalk-managed Transmission with 91.4-b/s/Hz Aggregate Spectral Efficiency// European Conference on Optical Communications Postdeadline Papers. - Amsterdam, Netherlands, 2012. – Th.3.C.1. - 1.-3.p.

73. Thyagarajan, K., Ghatak, A., *Fiber Optic Essentials* – USA: John Wiley & Sons, Inc., 2007. – 259.p.
74. Tomkos I., Hesse R., Antoniadis N., Boskovic A. Impact of filter concatenation on the performance of metropolitan area optical networks utilizing directly modulated lasers// *Optical Fiber Communication Conference Proceedings*. - Anaheim, CA, 2001. – 1.-3.p.
75. Venghaus H. *Wavelength Filters in Fiber Optics*. – USA: Springer, 2006. – 472.p.
76. Winzer P.J., Essiambre R.J. Advanced Modulation Formats for High-Capacity Optical Transport Networks// *J. Lightwave Technol.* – 2006. Vol.24. – 4711.-4728.p.
77. Winzer P.J., Pfennigbauer M., Strasser M.M., Leeb W.R. Optimum Filter Bandwidths for Optically Preamplified NRZ Receivers// *J. Lightwave Technol.* - 2001. – Vol.19(9), - 1263.–1273.p.
78. Xiong M., Ding Y.H., Zhang Q., Zhang X.L. All-optical clock recovery from 40 Gbit/s RZ signal based on microring resonators// *Appl. Opt.* – 2011. – Vol.50. – 5390.-5396.p.
79. Xiong M., **Ozoliņš O.**, Ding Y., Huang B., An Y., Ou H., Peucheret C., Zhang X. 41.6 Gb/s RZ-DPSK to NRZ-DPSK Format Conversion in a Microring Resonator// *17th Opto-Electronics and Communications Conference Technical Digest*. - Busan, Korea Republic, 2012. - 891.-892.p.
80. Xiong M., **Ozoliņš O.**, Ding Y., Huang B., An Y., Ou H., Peucheret C., Zhang X. Simultaneous RZ-OOK to NRZ-OOK and RZDPSK to NRZ-DPSK format conversion in a silicon microring resonator// *Opt. Exp.* – 2012. – Vol. 20, No. 25 – 27263.–27272.p.
81. Xu L., Chan J., Biberman A., Lira H.L.R., Lipson M., Bergman K. DPSK transmission through silicon microring switch for photonic interconnection networks// *IEEE Photon. Technol. Lett.* – 2011. – Vol.23. – 1103.-1105.p.
82. Xu L., Wang B.C., Baby V., Glesk I., Prucnal P.R. All optical data format conversion between RZ and NRZ based on a Mach Zehnder interferometric wavelength converter// *IEEE Photon. Technol. Lett.* – 2003. – Vol.5. – 308.-310.p.
83. Yariv A. Universal relations for coupling of optical power between microresonators and dielectric waveguides// *Electron. Lett.* – 2000. – Vol.36. 321.–322.p.
84. Yu Y., Zhang X. L., Huang D.X., Li L.J., Fu W. 20-Gb/s all-optical format conversions from RZ signals with different duty cycles to NRZ signals// *IEEE Photon. Technol. Lett.* – 2007. – Vol.19. – 1027.–1029.p.
85. Zhang L., Yang J.Y., Song M., Li Y., Zhang B., Beausoleil R.G., Willner A.E. Microring-based modulation and demodulation of DPSK signal// *Opt. Express*. – 2007. – Vol.15. – 11564.-11569.p.
86. Zhang Y., Xu, E.M. Huang D.X., Zhang X.L. All-optical format conversion from RZ to NRZ utilizing microfiber resonator// *IEEE Photon. Technol. Lett.* – 2009. – Vol.21. – 1202.–1204.p.
87. Zhang Z., Yu Y., Zhang X.L. Simultaneous all-optical demodulation and format conversion for multi-channel (CS)RZ-DPSK signals// *Opt. Express* – 2011. – Vol.19. – 12427.-12433.p.
88. Zhu B., Taunay T.F., Fishteyn M., Liu X., Chandrasekhar S., Yan M.F., Fini J.M., Monberg E.M., Dimarcello F.V. 112-Tbit/s Space-division multiplexed DWDM transmission with 14-b/s/Hz aggregate spectral efficiency over a 76.8-km seven-core fiber // *Optics Express*. – 2011. - Vol.19(17). – 16665.-16671.p.